

THESIS

DESIGN AND FABRICATION OF BIOACTIVE COATINGS TO CATALYTICALLY
GENERATE NITRIC OXIDE ON THE SURFACES OF EXTRACORPOREAL CIRCUITS

Submitted by

Tracey V. Wick

School of Biomedical Engineering

In partial fulfillment of the requirements

For the Degree of Master of Science

Colorado State University

Fort Collins, Colorado

Summer 2022

Master's Committee:

Advisor: Melissa M. Reynolds

Matthew Kipper

Christine Olver

Copyright by Tracey V. Wick 2022

All Rights Reserved

ABSTRACT

DESIGN AND FABRICATION OF BIOACTIVE COATINGS TO CATALYTICALLY GENERATE NITRIC OXIDE ON THE SURFACES OF EXTRACORPOREAL CIRCUITS

Blood-contacting medical devices suffer from biofouling caused by proteins, platelets and other cells adhering to the surface which often leads to severe complications and eventual device failure. In particular, extracorporeal membrane oxygenation (ECMO) is a life support treatment that is highly prone to coagulation issues due to a large blood-contacting surface area and turbulent blood flow. The ECMO circuits are constructed from catheters, tubing, and an oxygenator which all come into contact with blood and have several connections that alter the blood flow. The standard therapy to decrease thrombotic complications is to administer a systemic anticoagulant, usually unfractionated heparin. While this reduces clotting, harmful and potentially fatal hemorrhagic complications arise. Researchers have looked to nitric oxide (NO), a common biomolecule produced by the endothelium, as an alternative to locally inhibit clotting. Previous work has shown a reduction in thrombotic activity using NO-releasing substances, but these substances only last for a short period of time. An approach explored herein takes advantage of a catalytic mechanism to generate NO from endogenous NO-donors, *S*-nitrosothiols (RSNOs). RSNOs have been shown to catalytically generate NO through copper catalysis and in particular, with a copper-based metal-organic framework, $H_3[(Cu_4Cl)_3(BTtri)_8-(H_2O)_{12}] \cdot 72H_2O$ where $H_3BTtri = 1,3,5$ -tris(*1H*-1,2,3-triazole-5-yl)benzene] (CuBTtri). Importantly, CuBTtri has been shown to be stable under biological conditions and compatible with human cells; therefore, it is a promising candidate for biomedical applications. This report explores the

addition of CuBTTri on the surfaces of ECMO. In Chapter 2, a CuBTTri-doped composite is coated onto the extracorporeal circuitry tubing. The fabrication method to apply CuBTTri to the tubing is reported, and the coating was shown to actively generate NO when exposed to a RSNO and no adverse effects were noted during hemocompatibility testing. In Chapter 3, CuBTTri is immobilized on the surface of an ECMO oxygenator using polydopamine. The morphology of the coating was evaluated and the CuBTTri on the surface of the oxygenator was catalytically active, generating NO when exposed to a RSNO. The incorporation of CuBTTri on the surfaces of these components could improve the hemocompatibility of the device, providing a safer and more effective life support system.

ACKNOWLEDGEMENTS

Individual contributions and funding sources:

Chapter 2: H₃BT_{Tri} was synthesized by Jon Thai and Tracey V. Wick. GSNO was synthesized and characterized by Maga Mohnike. Alyssa C. Melvin and Tracey V. Wick contributed to experimental design and execution, data collection and analysis for all studies apart from the blood compatibility experiments. The data collection and analyzation for the blood compatibility experiments was completed by members of the Autonomous Reanimation and Evacuation Program (AREVA). George T. Harea and Yanyi Zang contributed to study execution and data analysis for the blood compatibility experiments. Andriy I. Batchinsky contributed to study conceptualization, funding acquisition, analysis validation. Teryn R. Roberts contributed to study conceptualization, experimental design and execution of the blood compatibility experiments. Melissa M. Reynolds contributed to study conceptualization and funding acquisition. All other work was carried out by Tracey V. Wick. This work was supported by the Assistant Secretary of Defense for Health Affairs endorsed by the Department of Defense, through the Peer Reviewed Medical Research Program – Technology/Therapeutic Development Award, under Award No. W81XWH-18-2-0048.

Chapter 3: H₃BT_{Tri} was synthesized by Jon Thai and Tracey V. Wick. GSNO was synthesized and characterized by Maga Mohnike. All other work was carried out by Tracey V. Wick.

TABLE OF CONTENTS

ABSTRACT.....	ii
ACKNOWLEDGEMENTS.....	iv
Chapter 1 – Introduction.....	1
1. Overview.....	1
2. Extracorporeal Membrane Oxygenation (ECMO).....	1
2.1 ECMO Circuit.....	1
2.2 ECMO Uses.....	2
3. Blood-Contacting Medical Devices.....	2
3.1 Complications Concerning Blood-Contacting Medical Devices.....	2
3.2 Strategies to Mitigate Coagulation on ECMO.....	3
4. Nitric Oxide (NO) Release from ECMO Components.....	4
5. Thesis Overview.....	6
Chapter 1 – References.....	8
Chapter 2 – Development and Blood Compatibility of a Stable Bioactive Metal-Organic Framework Composite Coating for Blood-Circulation Tubing.....	14
1. Introduction.....	14
2. Materials and Methods.....	16
2.1 Materials.....	16
2.2 CuBTTri Coating Procedure.....	17
2.2.1 CuBTTri Synthesis.....	17
2.2.2 Coating Procedure.....	18
2.2.3 Solvent Removal.....	19
2.3 CuBTTri Activity Analysis.....	20
2.4 Multi-day Coating Stability under Clinical Flow Conditions.....	21
2.4.1 Flow Stability Circuit Setup.....	21
2.4.2 Assessment of MOF Stability.....	22
2.4.3 Surface Imaging.....	22
2.5 Ex Vivo Blood Compatibility Testing (6 h) Under Clinical Flow Conditions.....	22
2.5.1 Hemocompatibility Circuit Setup.....	22
2.5.2 Donor Blood Collection.....	23
2.5.3 Blood Circulation and Hemocompatibility Tests.....	24

2.5.4 Post-Circulation Circuit Thrombus Assessment.....	26
2.5.5 Post-Circulation Tubing Activity Analysis.....	26
2.6 Statistical Analysis.....	27
3. Results and Discussion	27
3.1 Bioactive MOF Composite Coating Fabrication	28
3.1.1 Exploratory Coating Procedures	28
3.1.2 Solvent Removal.....	33
3.2 Tubing Activity Analysis	34
3.3 Evaluation of Coating Stability Under Flow Conditions	36
3.3.1 Delamination Testing.....	36
3.3.2 MOF Stability	40
3.4 Ex Vivo Blood Compatibility Testing (6 h) under Clinical Flow Conditions.....	43
3.4.1 Circuit Stability: Patency, Pump Performance, and Anticoagulation.....	44
3.4.2 Blood Stability: Cell Count and Chemistry	45
3.4.3 Blood Function: Platelet Activity and Tests of Coagulation	46
3.4.4 Post-Circulation Thrombus Deposition	49
3.4.5 Limitations.....	51
3.5 Stability and Activity Evaluation of Composite Coating After Blood Exposure	52
4. Conclusion	53
Chapter 2 – References	54
Chapter 3 – Surface Modification of Oxygenator Fibers with a Catalytically Active Metal- Organic Framework to Generate NO from GSNO	59
1. Introduction.....	59
2. Materials and Methods.....	61
2.1 Materials	61
2.2 CuBTTri Composite Preparation	62
2.2.1 CuBTTri Synthesis.....	62
2.2.2 Coating Procedure.....	63
2.3 Coating Characterization	64
2.4 Coating Activity Analysis.....	64
2.5 Multi-day Stability Testing.....	65
2.5.1 Assessment of MOF Stability in Saline	65

2.5.2 Assessment of MOF Activity After Stability Testing.....	65
2.6 Statistical Analysis.....	65
3. Results and Discussion	66
3.1 Coating Evaluation.....	66
3.2 Coating Activity Analysis.....	69
3.3 MOF Stability	70
4. Conclusion	72
Chapter 3 – References	74
Chapter 4 – Summary and Future Directions	79
1. General Conclusions	79
2. Conclusions and Future Work for the Tubing	79
3. Conclusions and Future Work for the Oxygenator	81

CHAPTER 1

INTRODUCTION

1. Overview

Extracorporeal organ support involves the circulation of blood through external medical devices providing assistance to the heart, lungs, kidneys, and/or liver. For example, hemodialysis mimics the functions of kidneys by filtering waste, water, and other ions to regulate blood pressure and hydration [1]. Extracorporeal liver support detoxifies and filters blood, while also metabolizing drugs and aiding in the digestive tract [2]. This report focusses on extracorporeal membrane oxygenation (ECMO), which provides cardiopulmonary support by externally oxygenating blood, and pumping it through the vasculature of the patient [3]. A major limitation of these extracorporeal circuits is the incidence of biofouling and thrombotic complications leading to device failure [4], [5]. Despite decades of research and technological advancements, extracorporeal circuits still have significant flaws and there is not a gold standard method to mitigate these issues. The study herein focuses on the incorporation of distinct surface coatings which have shown promise to potentially improve the hemocompatibility of these circuits.

2. Extracorporeal Membrane Oxygenation (ECMO)

2.1 ECMO Circuit

The three major components within the ECMO circuit are the oxygenator, a mechanical blood pump, and a heat exchanger all connected by medical tubing [6]. The centrifugal pump circulates blood through tubing and the vasculature of the patient if necessary, while the heat exchanger maintains the temperature of the blood [6]. The most important component of the ECMO circuit is the oxygenator, which provides respiratory support by maintaining gas

exchange. The hollow fibers within the oxygenator contain nanopores allowing the addition of oxygen and removal of carbon dioxide from blood [7]. This gas exchange is critical for the survival of the patient, as this will be the only oxygen provided to the rest of the body.

There are two distinct classifications of ECMO, veno-venous (VV-ECMO) and veno-arterial (VA-ECMO), which are administered based on the medical requirements of the patient. In both cases, a catheter is inserted into a major vein (usually the femoral vein or internal jugular vein) which drains deoxygenated blood from the vasculature of the patient [8]. The blood is returned either to the venous system (VV-ECMO) when pulmonary support is solely required, or the arterial system (VA-ECMO) if additional cardiovascular support is necessary, as this method will redirect the blood to the major arteries and skip pumping through the heart [9], [10].

2.2 ECMO Uses

ECMO is generally used as a last resort for patients in critical conditions. Most commonly, individuals who are in need of a heart or lung transplant or who are recovering from cardiac or pulmonary surgeries will be stabilized with ECMO [11], [12]. Additionally, critical conditions including acute respiratory distress syndrome (ARDS), congenital diaphragmatic hernia, other congenital lung disorders, cardiomyopathy, and myocarditis might require the use of ECMO, as well as neonates suffering from cardiac/respiratory failures [8], [13], [14].

Generally, ECMO is treated as a long-lasting life support system which might be required for days, weeks, or months depending on the severity of the condition [15].

3. Blood-Contacting Medical Devices

3.1 Complications Concerning Blood-Contacting Medical Devices

Biofouling and thrombosis complications associated with blood-contacting medical devices have been troubling researchers for decades, and there is yet to be a viable solution.

When blood comes into contact with a synthetic surface, like the components of ECMO, proteins, platelets, and cells to adhere and aggregate to the surface, promoting thrombus formation [5]. When enough biological material attaches to the surface, the medical device could fail, or thrombus formation could cause further catastrophic issues including embolism or stroke [16].

3.2 Strategies to Mitigate Coagulation on ECMO

The most common anticoagulation therapy to mitigate thrombotic complications while using extracorporeal life support is the administration of systemic anticoagulants, particularly unfractionated heparin. Unfractionated heparin binds to antithrombin, which enhances inhibitory activity preventing clotting [13]. Unfortunately, while unfractionated heparin reduces coagulation, hemorrhagic and excessive bleeding risks arise [17]. Hemorrhage occurring in the central nervous system is the leading cause of death while on ECMO [18] and occurs in 3%-12% of patients [19]. A method which inhibits localized clotting without causing systemic issues is greatly needed to improve the efficacy of the device.

Coating ECMO components is an encouraging idea and has been looked at for decades. In theory, coatings could change the properties of the local surface without causing systemic issues. In reality, this idea is very complex and a feasible, safe, and working coating has yet to be designed. There have been two general types of coatings developed, biopassive and bioactive [20]. Biopassive coatings focus on the surface properties, such as the hydrophilicity, to decrease protein adsorption whereas bioactive coatings provide some anticoagulant treatment. Coating albumin protein is one of the most common biopassive options, as this will increase the hydrophilicity of the surface and reduce alternative protein adsorption; however, this coating alone is not enough to completely inhibit thrombotic tendencies and additional systemic

coagulation is required [21]. The most common bioactive coating uses the immobilization of heparin on ECMO surfaces. While studies show heparin-based coatings help, additional systemic anticoagulation is still required and heparin often leaches from these coatings [22].

Coating the extracorporeal circuit components is challenging, and after decades of research there is not a working application. The most significant historical challenges include properly adhering the coating to the surface, maintaining the adhesion of the coating during aqueous and/or dynamic situations, and maintaining the performance of the device by not modifying the physical surface properties.

4. Nitric Oxide (NO) Release from ECMO Components

Investigators have looked to the endothelium for inspiration to develop an improved coating. Endothelial cells produce and secrete many inhibitory and activating molecules to prevent clot formation within blood vessels including nitric oxide (NO) [23]. NO has been extensively researched and it has been shown to aid in the inhibition of thrombus formation within the endothelium. NO is synthesized in endothelial cells from L-arginine and catalyzed by NO synthase [24]. Then, NO activates guanylate cyclase which will catalyze the formation of cyclic guanosine monophosphate (cGMP) from guanosine triphosphate (GTP) [25]. cGMP will enhance calcium ATPase, a transmembrane protein which removes calcium from the cells [26]. The reduction in cytosolic calcium suppresses P-selectin, a protein which mediates platelet adhesion, and glycoprotein IIb/IIIa, which binds soluble fibrinogen and aids in platelet aggregation [26]–[29]. The NO pathway to inhibit platelet adhesion and aggregation is biologically important and can be taken advantage of with medical device applications.

Given the localized anticoagulation properties of NO, previous attempts have been made to incorporate NO onto the surfaces of extracorporeal circuits. The most popular method is to

create a reservoir of a NO donating molecules within a polymeric matrix and coat this onto the surface of ECMO components. A proceeding reaction will release NO onto the surfaces of the extracorporeal circuit. This method is promising as a localized treatment for clotting as NO has a short half-life and will not interfere in the circulatory system of the patient [30], [31].

The most common NO donating molecules which have been coated onto extracorporeal circuitry components include *N*-Diazeniumdiolates, endogenous *S*-nitrosothiols (RSNOs), and nitrosyl metal complexes [32], [33]. Handa et al. incorporated a diazeniumdiolate species into extracorporeal circuitry tubing and found an attenuation in platelets and a reduction in blood clot area after undergoing a 4 h *in vivo* extracorporeal rabbit circuit [32]. However, the NO flux within the tubing only lasted 14 days and therefore might not be ideal for a longer lasting extracorporeal treatment [32]. Within that same research group, Goudie et al. incorporated a synthetically derived RSNO, *S*-nitroso-*N*-acetylpenicillamine (SNAP), with CarboSil into extracorporeal circuit tubing and found that the clotting time greatly decreased in an *in vivo* feline model; however, the study showed unsteady NO release rates within a 4 h study and the SNAP leached from the coating [33]. Other studies have also displayed RSNO leaching within coatings; this could be problematic and lead to large bursts of NO which could affect the coagulation of the blood in undesirable areas, for example within the patient's body [33].

Winnersbach et al. coated the oxygenator fibers with a NO-releasing hydrogel, and found the amount of platelets adhering to the fibers decreased after 48 minutes of *in vitro* blood exposure [34]. These studies showed promising anticoagulation results, but had their associated limitations, mainly due to the adhesion and stability of the coating and the longevity of the NO releasing material.

An important revelation with NO releasing materials was the incorporation of copper, as copper will catalyze the release of NO from RSNOs. Many researchers have developed coatings containing copper along with the addition of an RSNO to decrease thrombotic effects. Major et al. incorporated 80 nm copper nanoparticles into extracorporeal tubing; an *in vivo* rabbit model with an exogenous SNAP injection was used, and they found that platelet aggregation was reduced [35]. A potential problem with the model was that 234 ± 80 ng/mL of copper was leached, which could lead to copper toxicity. This group also incorporated *S*-nitrosoglutathione (GSNO) with copper nanoparticles into tubing and found a reduction in thrombus formation while maintaining platelet count [36]. Finally, Fan et al. reported the use of polydopamine (PDA) to immobilize a copper-based metal-organic framework (MOF), copper(II) benzene-1,3,5-tricarboxylate (CuBTC), on cardiovascular stents, and found sufficient NO release; however, the degradation properties of CuBTC released copper ions during this study [37]. Once again, the developed materials displayed anticoagulation results, but had limitations regarding the adhesion of the coatings.

5. Thesis Overview

Thrombotic complications need to be addressed in extracorporeal circuitry to provide safer and more effective life support. While systemic anticoagulation remains the standard to decrease clotting issues, new potentially fatal bleeding complications arise. Therefore, a technique which locally inhibits clotting could reduce coagulation and hemorrhagic complications. NO has been extensively researched as a localized anticoagulation therapy, and most of the literature incorporates NO releasing materials within the scaffold of the circuit component. The NO releasing materials have generally shown a decrease in thrombotic complications or a reduction in platelet function; however, these therapies only last for a short

period of time (up to a couple of weeks at most) and sometimes leach molecules when exposed to aqueous solutions; therefore, they might not be the optimal solution.

Within this thesis, I have developed coatings using a copper-based metal-organic framework (MOF), $H_3[(Cu_4Cl)_3-(BTri)_8]$, $H_3BTri = 1,3,5\text{-tris}(1H\text{-}1,2,3\text{-triazole-}5\text{-yl)benzene]$ (CuBTri) for ECMO circuitry which has never been done before. CuBTri was chosen because it has been shown to generate NO from RSNOs using a catalytic mechanism [38], [39] and importantly, is water-stable and compatible with cells making it a promising candidate to use in medical devices [40]. The major objectives of the project were to 1) adhere the CuBTri onto ECMO components, 2) maintain this adhesion during dynamic aqueous environments, and 3) confirm the generation of NO when the coating is exposed to an endogenous RSNO. Chapter 2 describes the coating method to apply CuBTri onto standard ECMO tubing and the initial stability and activity results from this coating. In brief, the CuBTri was successfully integrated onto the tubing and was determined to adequately generate NO in the presence of an endogenous RSNO. The coating itself remained stable, but there is a possibility that the CuBTri degrades when exposed to shear forces, and further experimentation will have to be done to assess the stability of CuBTri. Chapter 3 describes the coating method to apply CuBTri onto oxygenator fibers and the initial stability and activity results. In brief, the CuBTri was successfully immobilized on the fibers and coating was shown to generate NO when exposed to an endogenous RSNO. Similarly to the tubing, the coating itself remained stable when exposed to an aqueous dynamic environment, but more experimentation is needed to properly assess the stability of the MOF. This project demonstrates the ability to coat ECMO components with CuBTri for the ultimate goal of preventing thrombus formation.

CHAPTER 1

REFERENCES

- [1] “Hemodialysis | NIDDK,” *National Institute of Diabetes and Digestive and Kidney Diseases*. <https://www.niddk.nih.gov/health-information/kidney-disease/kidney-failure/hemodialysis> (accessed May 25, 2022).
- [2] T. Wiesmann, D. Hoenl, H. Wulf, and M. Iqrsusi, “Extracorporeal liver support: trending epidemiology and mortality - a nationwide database analysis 2007–2015,” *BMC Gastroenterology*, vol. 19, no. 1, p. 160, Sep. 2019, doi: 10.1186/s12876-019-1077-y.
- [3] J. F. Fraser *et al.*, “ECMO – the clinician’s view,” *ISBT Science Series*, vol. 7, no. 1, pp. 82–88, 2012, doi: 10.1111/j.1751-2824.2012.01560.x.
- [4] K. Giuliano *et al.*, “Extracorporeal Membrane Oxygenation Complications in Heparin- and Bivalirudin-Treated Patients,” *Crit Care Explor*, vol. 3, no. 7, p. e0485, Jul. 2021, doi: 10.1097/CCE.0000000000000485.
- [5] J. L. Harding and M. M. Reynolds, “Combating medical device fouling,” *Trends in Biotechnology*, vol. 32, no. 3, pp. 140–146, Mar. 2014, doi: 10.1016/j.tibtech.2013.12.004.
- [6] L. Lequier, S. B. Horton, D. M. McMullan, and R. H. Bartlett, “Extracorporeal Membrane Oxygenation Circuitry,” *Pediatr Crit Care Med*, vol. 14, no. 5 0 1, pp. S7-12, Jun. 2013, doi: 10.1097/PCC.0b013e318292dd10.
- [7] J. M. Daniel *et al.*, “Hollow Fiber Oxygenator Composition Has a Significant Impact on Failure Rates in Neonates on Extracorporeal Membrane Oxygenation: A Retrospective Analysis,” *J Pediatr Intensive Care*, vol. 7, no. 1, pp. 7–13, Mar. 2018, doi: 10.1055/s-0037-1599150.

- [8] S. F. Marasco, G. Lukas, M. McDonald, J. McMillan, and B. Ihle, “Review of ECMO (Extra Corporeal Membrane Oxygenation) Support in Critically Ill Adult Patients,” *Heart, Lung and Circulation*, vol. 17, pp. S41–S47, Jan. 2008, doi: 10.1016/j.hlc.2008.08.009.
- [9] E. Pavlushkov, M. Berman, and K. Valchanov, “Cannulation techniques for extracorporeal life support,” *Ann Transl Med*, vol. 5, no. 4, p. 70, Feb. 2017, doi: 10.21037/atm.2016.11.47.
- [10] H. Appelt *et al.*, “Factors associated with hemolysis during extracorporeal membrane oxygenation (ECMO)-Comparison of VA- versus VV ECMO,” *PLoS One*, vol. 15, no. 1, p. e0227793, 2020, doi: 10.1371/journal.pone.0227793.
- [11] M. M. Kittleson *et al.*, “Heart transplant recipients supported with extracorporeal membrane oxygenation: outcomes from a single-center experience,” *J Heart Lung Transplant*, vol. 30, no. 11, pp. 1250–1256, Nov. 2011, doi: 10.1016/j.healun.2011.05.006.
- [12] E. Faccioli *et al.*, “Extracorporeal membrane oxygenation in lung transplantation: Indications, techniques and results,” *World J Transplant*, vol. 11, no. 7, pp. 290–302, Jul. 2021, doi: 10.5500/wjt.v11.i7.290.
- [13] R. Barton, V. Ignjatovic, and P. Monagle, “Anticoagulation during ECMO in neonatal and paediatric patients,” *Thrombosis Research*, vol. 173, pp. 172–177, Jan. 2019, doi: 10.1016/j.thromres.2018.05.009.
- [14] P. P. O’Rourke *et al.*, “Extracorporeal Membrane Oxygenation and Conventional Medical Therapy in Neonates With Persistent Pulmonary Hypertension of the Newborn: A Prospective Randomized Study,” *Pediatrics*, vol. 84, no. 6, pp. 957–963, Dec. 1989, doi: 10.1542/peds.84.6.957.

- [15] M. M. G. Mulder, I. Fawzy, and M. D. Lancé, “ECMO and anticoagulation: a comprehensive review,” vol. 26, no. 1, p. 8, 2018.
- [16] I. H. Jaffer and J. I. Weitz, “The blood compatibility challenge. Part 1: Blood-contacting medical devices: The scope of the problem,” *Acta Biomaterialia*, vol. 94, pp. 2–10, Aug. 2019, doi: 10.1016/j.actbio.2019.06.021.
- [17] Hwa Jin Cho, Do Wan Kim, Gwan Sic Kim, and In Seok Jeong, “Anticoagulation Therapy during Extracorporeal Membrane Oxygenator Support in Pediatric Patients,” *Chonnam Medical Journal*, vol. 53, no. 2, pp. 110–117, May 2017, doi: 10.4068/cmj.2017.53.2.110.
- [18] Y. A. Cavayas, L. del Sorbo, and E. Fan, “Intracranial hemorrhage in adults on ECMO,” *Perfusion*, vol. 33, no. 1_suppl, pp. 42–50, May 2018, doi: 10.1177/0267659118766435.
- [19] R. C. Reed and J. C. Rutledge, “Laboratory and Clinical Predictors of Thrombosis and Hemorrhage in 29 Pediatric Extracorporeal Membrane Oxygenation Nonsurvivors,” *Pediatr Dev Pathol*, vol. 13, no. 5, pp. 385–392, Sep. 2010, doi: 10.2350/09-09-0704-OA.1.
- [20] M. Zhang *et al.*, “Anti-thrombogenic Surface Coatings for Extracorporeal Membrane Oxygenation: A Narrative Review,” *ACS Biomater. Sci. Eng.*, vol. 7, no. 9, pp. 4402–4419, Sep. 2021, doi: 10.1021/acsbmaterials.1c00758.
- [21] T. M. Maul, M. P. Massicotte, and P. D. Wearden, *ECMO Biocompatibility: Surface Coatings, Anticoagulation, and Coagulation Monitoring*. IntechOpen, 2016. doi: 10.5772/63888.
- [22] A. Ontaneda and G. M. Annich, “Novel Surfaces in Extracorporeal Membrane Oxygenation Circuits,” *Front Med (Lausanne)*, vol. 5, p. 321, Nov. 2018, doi: 10.3389/fmed.2018.00321.
- [23] M. M. Reynolds and G. M. Annich, “The artificial endothelium,” *Organogenesis*, vol. 7, no. 1, pp. 42–49, Mar. 2011, doi: 10.4161/org.7.1.14029.

- [24] D. J. Stuehr, “Enzymes of the L-Arginine to Nitric Oxide Pathway,” *The Journal of Nutrition*, vol. 134, no. 10, pp. 2748S-2751S, Oct. 2004, doi: 10.1093/jn/134.10.2748S.
- [25] Z. Nong, M. Hoylaerts, N. Van Pelt, D. Collen, and S. Janssens, “Nitric Oxide Inhalation Inhibits Platelet Aggregation and Platelet-Mediated Pulmonary Thrombosis in Rats,” *Circulation Research*, vol. 81(5), pp. 865–869, Nov. 1997, doi: 10.1161/01.RES.81.5.865.
- [26] J. Loscalzo, “Nitric Oxide Insufficiency, Platelet Activation, and Arterial Thrombosis,” *Circulation Research*, vol. 88, no. 8, pp. 756–762, Apr. 2001, doi: 10.1161/hh0801.089861.
- [27] D. Varga-Szabo, A. Braun, and B. Nieswandt, “Calcium signaling in platelets,” *Journal of Thrombosis and Haemostasis*, vol. 7, no. 7, pp. 1057–1066, 2009, doi: 10.1111/j.1538-7836.2009.03455.x.
- [28] A. Smolenski, “Novel roles of cAMP/cGMP-dependent signaling in platelets,” *Journal of Thrombosis and Haemostasis*, vol. 10, no. 2, pp. 167–176, 2012, doi: 10.1111/j.1538-7836.2011.04576.x.
- [29] M. Merten and P. Thiagarajan, “P-Selectin Expression on Platelets Determines Size and Stability of Platelet Aggregates,” *Circulation*, vol. 102, no. 16, pp. 1931–1936, Oct. 2000.
- [30] D. Giustarini, A. Milzani, R. Colombo, I. Dalle-Donne, and R. Rossi, “Nitric oxide and S-nitrosothiols in human blood,” *Clinica Chimica Acta*, vol. 330, no. 1, pp. 85–98, Apr. 2003, doi: 10.1016/S0009-8981(03)00046-9.
- [31] J. P. Wallis, “Nitric oxide and blood: a review,” *Transfusion Medicine*, vol. 15, no. 1, pp. 1–11, 2005, doi: 10.1111/j.1365-3148.2005.00542.x.
- [32] H. Handa *et al.*, “In vitro and in vivo study of sustained nitric oxide release coating using diazeniumdiolate-doped poly(vinyl chloride) matrix with poly(lactide-co-glycolide)

- additive,” *J. Mater. Chem. B*, vol. 1, no. 29, pp. 3578–3587, Jul. 2013, doi: 10.1039/C3TB20277A.
- [33] M. J. Goudie, B. M. Brainard, C. W. Schmiedt, and H. Handa, “Characterization and in vivo performance of nitric oxide-releasing extracorporeal circuits in a feline model of thrombogenicity,” *Journal of Biomedical Materials Research Part A*, vol. 105, no. 2, pp. 539–546, 2017, doi: 10.1002/jbm.a.35932.
- [34] P. Winnersbach *et al.*, “Endogenous Nitric Oxide-Releasing Microgel Coating Prevents Clot Formation on Oxygenator Fibers Exposed to In Vitro Blood Flow,” *Membranes (Basel)*, vol. 12, no. 1, p. 73, Jan. 2022, doi: 10.3390/membranes12010073.
- [35] T. C. Major *et al.*, “The hemocompatibility of a nitric oxide generating polymer that catalyzes S-nitrosothiol decomposition in an extracorporeal circulation model,” *Biomaterials*, vol. 32, no. 26, pp. 5957–5969, Sep. 2011, doi: 10.1016/j.biomaterials.2011.03.036.
- [36] M. E. Douglass *et al.*, “Catalyzed Nitric Oxide Release via Cu Nanoparticles Leads to an Increase in Antimicrobial Effects and Hemocompatibility for Short-Term Extracorporeal Circulation,” *ACS Appl. Bio Mater.*, vol. 2, no. 6, pp. 2539–2548, Jun. 2019, doi: 10.1021/acsabm.9b00237.
- [37] Y. Fan *et al.*, “Immobilization of nano Cu-MOFs with polydopamine coating for adaptable gasotransmitter generation and copper ion delivery on cardiovascular stents,” *Biomaterials*, vol. 204, pp. 36–45, Jun. 2019, doi: 10.1016/j.biomaterials.2019.03.007.
- [38] R. R. Tuttle, H. N. Rubin, C. D. Rithner, R. G. Finke, and M. M. Reynolds, “Copper ion vs copper metal–organic framework catalyzed NO release from bioavailable S-Nitrosoglutathione en route to biomedical applications: Direct ¹H NMR monitoring in

water allowing identification of the distinct, true reaction stoichiometries and thiol dependencies,” *Journal of Inorganic Biochemistry*, vol. 199, p. 110760, Oct. 2019, doi: 10.1016/j.jinorgbio.2019.110760.

[39] J. L. Harding and M. M. Reynolds, “Composite materials with embedded metal organic framework catalysts for nitric oxide release from bioavailable S-nitrosothiols,” *J. Mater. Chem. B*, vol. 2, no. 17, pp. 2530–2536, Apr. 2014, doi: 10.1039/C3TB21458C.

[40] M. J. Neufeld, B. R. Ware, A. Lutzke, S. R. Khetani, and M. M. Reynolds, “Water-Stable Metal–Organic Framework/Polymer Composites Compatible with Human Hepatocytes,” *ACS Appl. Mater. Interfaces*, vol. 8, no. 30, pp. 19343–19352, Aug. 2016, doi: 10.1021/acsami.6b05948.

CHAPTER 2
DEVELOPMENT AND BLOOD COMPATIBILITY OF A STABLE BIOACTIVE METAL-
ORGANIC FRAMEWORK COMPOSITE COATING FOR BLOOD-CIRCULATION
TUBING

1. Introduction

A class of extracorporeal medical devices involves circulation of blood through a device outside of the patient's body to perform the functions of vital organs including lungs, heart, liver, and/or kidneys. A major limitation of these extracorporeal systems is the incidence of associated thrombotic and bleeding complications [1]. This is due to the extensive surface area of artificial plastics that contact blood during therapy, as well as the non-physiological blood flow conditions that occur in the extracorporeal device circuit [2].

When blood contacts an extracorporeal circuit, plasma protein adsorption rapidly occurs on the hydrophobic plastics, forming an intermediate layer for deposition of thrombi on the biomaterial surface [3]. Both coagulation of blood plasma and platelet-mediated interactions contribute to thrombus formation. These thrombi can alter device performance by impeding blood flow and/or affecting device function; and can also result in coagulopathic and pro-inflammatory complications to the patient [4]. The current clinical practice to prevent clot formation during extracorporeal circulation is to administer systemic anticoagulants during therapy, such as unfractionated heparin; however, anticoagulation in these patients results in frequent bleeding complications that can be fatal [5]. Immobilization of the anticoagulant heparin on the artificial surfaces of extracorporeal organ support devices is frequently utilized to attempt to minimize clot deposition locally; however, this approach has not proven to be

effective in the absence of systemic anticoagulation [2]. Furthermore, systemic and immobilized heparin can cause heparin-induced thrombocytopenia (HIT), an adverse immune-mediated drug reaction caused by antibodies that bind to and activate platelets. This recently occurred in a COVID-19 patient that received extracorporeal circulation for lung support in the absence of systemic heparin with a heparin-coated lung support device [6].

To address these coagulopathic complications, researchers have looked to the endogenous vascular endothelium for inspiration. In the healthy vasculature, nitric oxide (NO) is a potent signaling molecule that is continuously released and performs numerous antithrombotic functions [7]. NO reversibly inhibits platelet activation and aggregation at the endothelial surface, prevents monocyte activation, and also has antimicrobial properties [8]. For this reason, NO is a promising target for blood-contacting biomaterial applications as it can provide localized inhibition of platelet activation and aggregation at the artificial surface, without inhibiting platelet activation in the patient's systemic circulation [2]. Due to these promising antithrombotic properties of NO, we explore the use of a metal-organic framework (MOF) composite coating on extracorporeal circuit tubing as a catalyst for NO generation to inhibit blood clotting.

MOFs are porous crystalline coordination compounds built from metal centers and organic linkers. They have been shown to be useful in a variety of applications including gas storage, separation, drug delivery, and catalysis [9]. In recent years, a copper-based MOF, $H_3[(Cu_4Cl)_3(BTtri)_8-(H_2O)_{12}] \cdot 72H_2O$ where $H_3BTtri = 1,3,5$ -tris(*1H*-1,2,3-triazole-5-yl)benzene] (CuBTtri), has been shown to be an effective catalyst to generate NO from *S*-nitrosothiols (RSNOs), a group of biologically occurring NO-donating compounds [10].

Importantly, CuBTri has been shown to be stable under biological conditions and compatible with human cells, which makes it a promising compound for medical applications [11].

The objective of this study was to engineer and evaluate the application of CuBTri to medical grade Tygon tubing of the same grade and dimension that is frequently utilized for extracorporeal lung support applications. We developed a fabrication method to apply CuBTri to extracorporeal circulation tubing, and then evaluated whether the coating was stable, active, and blood compatible under flow conditions that are clinically utilized during extracorporeal lung support. We hypothesized the coating is stable when applied to extracorporeal circulation tubing without eliciting harmful effects, when evaluated using swine blood.

We have developed a process to dispersedly coat CuBTri on Tygon tubing used in extracorporeal circuitry and have shown that the CuBTri within the coating actively generates NO. It is important that the CuBTri particles are dispersed throughout the coating, so catalysis of NO occurs across the entire surface. If there is a cluster of settled MOF particles in one section of the tubing and a lack of particles in another, this could result in an inconsistent distribution of NO generation leading to localized clotting. Additionally, the coating was stable during fluid flow, meaning that the polymeric composite did not delaminate or sustain any damage. Finally, the CuBTri within the coating was shown to be active, generating NO when exposed to a biologically relevant concentration of GSNO.

2. Materials and Methods

2.1 Materials

All reagents and solvents were purchased from vendors and were used as stated in this chapter. 1,3,5-triethynylbenzene (98%) and copper(II) chloride dihydrate (99%, $\text{CuCl}_2 \cdot \text{H}_2\text{O}$) were purchased from Alfa Aesar (Ward Hill, MA). Copper(I) iodide (>99.5%, CuI) was

purchased from Sigma-Aldrich (St. Louis, MO). Methanol (99.9%) and sodium chloride (99.0%) were purchased from Fisher Scientific (Hampton, NH). Diethyl ether (>99.0%) was purchased from Millipore Sigma (Burlington, MA). Tetrahydrofuran (99.0%, THF) and N,N-dimethylformamide (99.8%, DMF) were purchased from VWR International (Radnor, PA). Trimethylsilyl azide (>95.0%) was purchased from Tokyo Chemical Industry (Tokyo, Japan). Ultrapure water (18.2 M Ω ·cm) was supplied from Millipore MilliQ-IQ water purification system (Billerica, MA).

The three types of tubing that were purchased were Pumpsil pump tubing (Pumpsil #36, Falmouth, United Kingdom), clear polyvinyl chloride tubing (Fisher Scientific, 141697J, Waltham, MA) with an inner diameter (ID) of 1/2", and Tygon tubing (Saint-Gobain, ND-100-65, Courbevoie, France) with 3/8" inner diameter was purchased to be coated. Identical Tygon tubing was purchased to be cut up and used as the Tygon polymer.

2.2 *CuBTTri Coating Procedure*

2.2.1 *CuBTTri Synthesis*

$\text{H}_3[(\text{Cu}_4\text{Cl})_3(\text{BTTri})_8(\text{H}_2\text{O})_{12}] \cdot 72\text{H}_2\text{O}$ (CuBTTri) was synthesized using a previously reported method [12]. Briefly, 1,3,5-triethynylbenzene (5.3 g, 35.29 mmol) and CuI (1.011 g, 5.31 mmol) were added to a solution of DMF (180 mL) and methanol (20 mL) and mixed under a nitrogen atmosphere. Trimethylsilyl azide (21 mL, 158.95 mmol) was added, and the reaction was heated to 100°C for 36-48 h. Excess solvent was removed with rotary evaporation. The precipitate, 1,3,5-tris(1H-1,2,3-triazol-5-yl)-benzene (H₃BTTri), was collected via filtration then washed with 500 mL each of H₂O and diethyl ether.

A solution of H₃BTTri (1.2375 g, 5.1535 mmol) and DMF (220 mL) was sonicated for 1 h. CuCl₂·H₂O (2.1065 g, 12.36 mmol) was added to the mixture then heated to 100°C for 72 h.

The final CuBTTri product, a purple precipitate, was collected using a fine porosity fritted glass funnel and washed with 100 mL each of DMF and water. The filtered solid was heated in 200 mL of water for 24 h at 95°C. The solid was filtered, washed with 100 mL of water, and heated for 24 h at 95 °C three separate times. After the final water wash, the product was dried under a partial vacuum then hand-ground for 10 min.

2.2.2 Coating Procedure

The methods for the final coating procedure are outlined within this section. More details of the different coating iterations are outlined in the Results section. To coat each tubing segment, a coating solution was prepared with CuBTTri and Tygon polymer in THF based on previous research by Zang [13]. Separate coating solutions with two concentrations of CuBTTri, 1.0% w/v and 0.1% w/v, were prepared to coat Tygon extracorporeal circulation tubing. These coatings were further evaluated and compared to determine which concentration of CuBTTri is ideal.

A 60 mL coating solution containing CuBTTri and Tygon polymer in THF was used to coat 7 feet of Tygon tubing. A Tygon solution was prepared by dissolving 0.60 g Tygon polymer in 30 mL THF and stirred overnight. The next day, either 0.6 g or 0.06 g CuBTTri (for the 1.0% w/v formulation or the 0.1% w/v formulation respectively) was added to 30 mL of THF. This solution was stirred rapidly for 20 min and sonicated (Branson, 3800 Ultrasonic Cleaner, Brookfield, CT) for 30 min. The Tygon solution was added to this solution then stirred for 20 min and sonicated for 30 min to fully suspend the CuBTTri in solution. This formed the coating solution which consisted of 1.0% w/v Tygon and either 1.0% w/v or 0.1% w/v CuBTTri.

The coating application system setup is displayed in Figure 2.1. One end of the 7-foot Tygon tubing was connected to a 22" segment of 3/8" ID pump tubing (Pumpsil #36, Falmouth,

United Kingdom) which was inserted through the peristaltic pump (Watson Marlow, 9131, Falmouth, United Kingdom). A 1/2" ID tubing (Fisher, 14-169-7J, Hampton, NH) was connected to the other end of the Tygon tubing with a clamp for the coating solution to be poured into. Additionally, this end of the Tygon tubing was elevated 8" to increase the flow rate of the coating solution. After the 60 mL coating solution was poured into the 1/2" ID tubing, the clamp was released, and the peristaltic pump was turned on to 175 rpm (2.646 L/min). The coating solution flowed through the tubing and waste was collected at the end. The newly coated Tygon extracorporeal circulation tubing was then rotated horizontally on a mechanical rotator (IKA, RW 20 Digital, Wilmington, NC) for 5 min to prevent unwanted settling of CuBTtri particles.

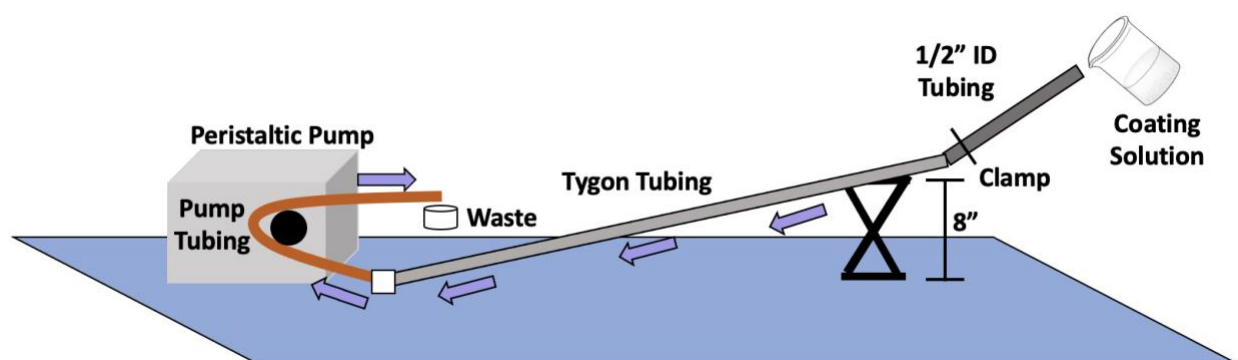


Figure 2.1. CuBTtri Tubing Application Setup. A peristaltic pump was used to pump the coating solution from one end of the Tygon tubing to the other, which coated the interior surface area of the Tygon tubing.

2.2.3 Solvent Removal

Following coating application, tubing was placed under high vacuum at 60 °C to remove excess THF. An Agilent 8890 Gas Chromatograph System (GC) with an Agilent DB-624 fused silica column (20 m length, 180 µm ID, 1 µm film thickness) equipped with a 7679A Headspace Sampler (Santa Clara, CA) was used to measure THF content. To prepare the samples for analysis, a 1 cm piece of coated Tygon tubing was cut lengthwise and added to a 20 mL

headspace vial (Agilent, 5182-0839, Santa Clara, CA) containing 5 mL of DMF. The vial was held in the Headspace Sampler at 70 °C with minor agitation for 20 min prior to injection to extract any residual THF in the coating. A sample of the vial headspace (0.5 s injection duration) was injected into the GC (240 °C injector temperature, split ratio 75, split flow 97.5 mL/min) with a helium carrier gas at a flow rate of 1.3 mL/min. The oven was held at an initial temperature of 45 °C for 1.5 min then ramped to 90 °C at a rate of 25 °C/min. At 90 °C the rate was increased to 35 °C/min until reaching a final temperature of 200 °C. The flame ionization detector (FID) was set to 240 °C with air flow of 400 mL/min, hydrogen flow of 40 mL/min, and make-up gas flow of 25 mL/min. A 6-point calibration curve was generated with concentrations 0.0005-0.1 v/v% THF in DMF. Our method had a detection limit of 3.466×10^{-6} % (v/v), linear range of 1.156×10^{-5} – 1.0784×10^{-1} % (v/v) ($R^2 = 0.99998$), and sensitivity of 1.5916×10^4 pA·s/% (v/v) with THF eluting at 2.700 min. The tubing was used for further experiments only if no THF was detected (<DL).

2.3 CuBTTri Activity Analysis

Tubing segments were collected for assessment of CuBTTri catalytic activity. GSNO oxidation by CuBTTri in the composite was used to evaluate the activity of the coatings after the solvent was removed. Nitric Oxide Analyzers (280i, Zysense, Weddington, North Carolina) were used to track GSNO oxidation via chemiluminescence-based NO detection. Millipore water was added to the reaction cell for a final volume of 5 mL. After beginning the experiment, 10 μM GSNO was injected into the reaction cell. The reaction proceeded at 38°C shielded from light with constant nitrogen bubbling with a collection interval of 1 s. NO fluxes were calculated by using the average flux in the experiment between after the initial spike in NO release and before

the NO dropped down to 0. This was due to the reaction maintaining stable NO release for a period of time.

2.4 Multi-day Coating Stability under Clinical Flow Conditions

2.4.1 Flow Stability Circuit Setup

A schematic for the coating stability evaluation is shown in Figure 2.2 using 38 °C saline (4.5 g sodium chloride in 500 mL water). A 3 ft segment of coated Tygon tubing was attached to pump tubing on both sides using connectors (Dynalon, 227245, Rochester, NY). Both 24 h and 72 h experiment were performed. For the 24-h experiment, saline was pumped through the tubing for 24 h at 2.5 L/min (n=3). For the 72-h experiment, saline was pumped through the tubing at 1 L/min for 24 h, then 2 L/min for the next 24 h, and 2.5 L/min for the final 24 h (n=3). These flow rates were selected to replicate commonly utilized blood flow rates for extracorporeal partial lung support applications, such as extracorporeal carbon dioxide removal (ECCO₂R) [14].

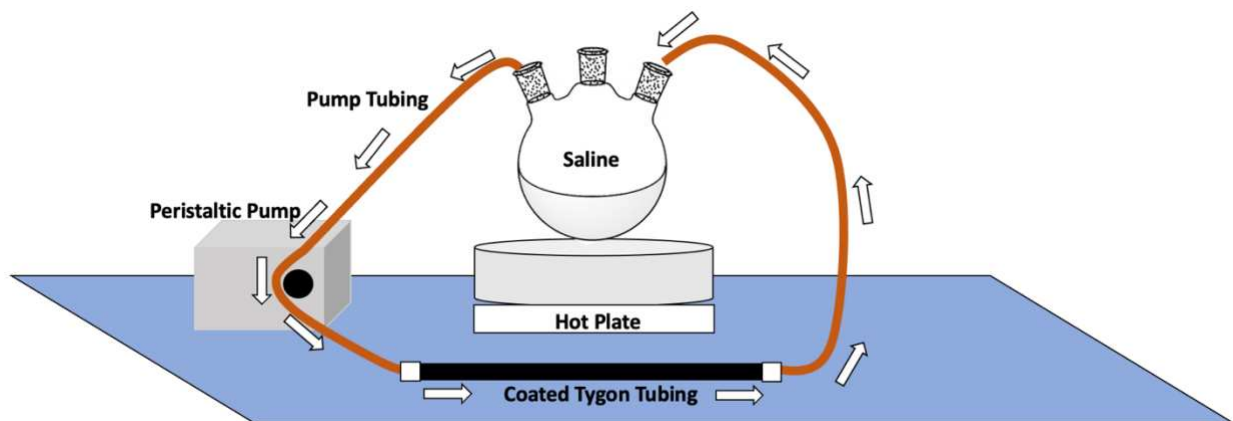


Figure 2.2. Flow Experiment used to determine the stability of the MOF composite coating. A peristaltic pump was used to circulate 38 °C saline continuously through the coated Tygon tubing.

2.4.2 Assessment of MOF Stability

Inductively coupled plasma mass spectroscopy (ICP-MS, NexION 350D, PerkinElmer, Waltham, MA) was used to evaluate the stability of CuBTri during flow circuits. A sample of the saline solution was collected after every 24-h period from the circuit and analyzed using ICP-MS for copper detection (n=3 at each time period).

2.4.3 Surface Imaging

At regular 24 h intervals during multi-day coating stability tests, segments of CuBTri coated Tygon were collected for assessment of coating stability via scanning electron microscopy (SEM) imaging (n=3 samples). A JEOL JSM-6500F scanning electron microscope (Akishima, Tokyo, Japan) was used with an accelerating voltage of 15.0 kV at magnifications of 100x. The samples were sputter-coated with 20 nm of gold before imaging.

2.5 Ex Vivo Blood Compatibility Testing (6 h) Under Clinical Flow Conditions

2.5.1 Hemocompatibility Circuit Setup

The following blood procedures were performed by the Autonomous Reanimation and Evacuation Research Program (AREVA, San Antonio, TX, USA) who generously shared their methods and results to determine the hemocompatibility of the coating. 0.1% w/v CuBTri-coated Tygon tubing was incorporated into a benchtop blood circulation loop consisting of 2 segments of tubing (~3.3 feet [1 m] length, 3/8" ID), a blood reservoir which stored the collected swine blood, and a clinical centrifugal blood pump for extracorporeal lung support (DP3 pump head and Novalung Console, Xenios/Fresenius Medical Care; Bad Homburg, Germany) as seen in Figure 2.3. Control circulation loops (CTRL) were constructed using unmodified Tygon ND-100-65 tubing. Blood flow rate in the circulation loops was monitored using clamp-on ultrasonic flow sensors (Transonic Systems; Ithaca, NY, USA); and a Hemotherm heating system

(Gentherm Medical; Cincinnati, OH, USA) was used to maintain circuit temperature (38 °C). For each experiment (n=4), 2 CuBTri circulation loops and 2 CTRL circulation loops were tested simultaneously with blood from one donor (n=8 circuits/group). All circuits were primed with 500 mL normal saline at 1.5 L/min flow rate for 30 min prior to start of blood testing.

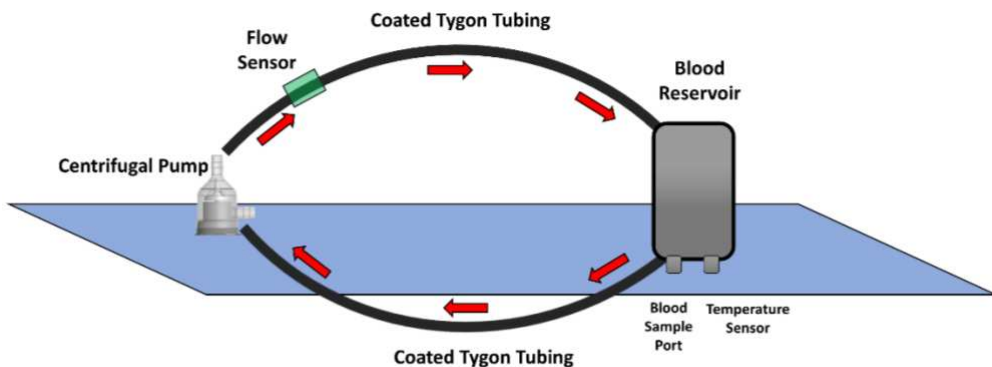


Figure 2.3. Hemocompatibility Circuit Setup. A benchtop blood circulation loop was constructed to assess the blood compatibility of CuBTri tubing. The loop consisted of two ~3.3 foot (1 m) segments of Tygon® tubing (either CuBTri-coated or unmodified), which were connected on one end to a blood reservoir and on the other end to a centrifugal blood pump. Heparinized swine donor blood was circulated through the loop at a blood flow rate of 1.5 L/min for 6 h.

2.5.2 Donor Blood Collection

Blood was collected following approved protocols (SU001-10-22 and SU003-09-23, University of Texas San Antonio, San Antonio, TX, USA) at the Autonomous Reanimation and Evacuation Research Program (AREVA, San Antonio, TX, USA) in compliance with the Animal Welfare Act, the principles set forth in the “Guide for the Care and Use of Laboratory Animals,” and all local, state and federal guidelines for the ethical use of animals. Blood (2 L) was collected from anesthetized, mechanically ventilated Yorkshire swine donors (54 ± 3 kg) that

were subjects in an unrelated study involving polytrauma injury. Swine donors were not anticoagulated, and blood was collected at 24-72 hours post-polytrauma injury. Importantly, the use of blood from subjects that encountered trauma increases the clinical relevancy of our experimental design, as subjects that receive extracorporeal organ support frequently have underlying coagulopathic complications that contribute to bleeding and thrombosis during therapy [1]. Blood was collected into a collection bag in low-dose unfractionated heparin (0.75 U/mL) and was then immediately divided between four circulations loops (2 CuBTri loops, 2 CTRL loops; 500 mL blood/loop).

2.5.3 Blood Circulation and Hemocompatibility Tests

Blood circulation was initiated and maintained at 1.5 L/min throughout the 6-h study to simulate flow conditions during extracorporeal therapy for partial lung support. During circulation, heparin boluses (25-50 U) were administered if necessary for anticoagulation to maintain an activated clotting time (ACT) of 125-160 s. This target range was selected to achieve less-than or similar degree of anticoagulation as is used clinically during ECLS. At start of circulation (BL) and hourly, blood samples were collected to assess ACT, blood gases, methemoglobin fraction and chemistry (potassium and lactate concentration). Blood pump revolutions per min required to maintain the flow rate and total quantity of heparin bolused to maintain the ACT target were recorded.

Additional blood samples were collected at baseline, and at 3- and 6-h to assess blood stability and coagulation function. Blood was collected into tubes containing ethylenediaminetetraacetic acid (EDTA) for assessment of CBC (Advia 2120, Siemens; Munich, Germany), platelet activation panel and plasma-free hemoglobin. Citrated blood (3.2%) was collected for assessment of thromboelastography, platelet aggregometry, and coagulation tests.

For platelet activation assessment, a flow cytometry panel (CytoFLEX, Beckman Coulter; Brea, CA, USA) was performed as previously reported [15]. Monoclonal antibodies were used to identify the platelet population in whole blood (CD61-FITC, clone JM2E5; Bio-Rad; Hercules, CA, USA) that was in an active configuration, defined by expression of P-selectin on the platelet surface (CD62-RPE, clone Psel.KO.2.5, Bio-Rad; Hercules, CA, USA). To identify platelets in a procoagulant configuration, bovine lacatdherin-Alexafluor 647 (Haemotologic Technologies, Inc; Essex Junction, VT, USA) was used to indicate phosphatidyl serine expression.

Thromboelastography (TEG 5000; Haemonetics Corporations Braintree, MA, USA) was performed using whole blood and the citrated kaolin assay with heparinase cups per manufacturer's instructions. Platelet aggregation was assessed as previously reported using whole blood impedance aggregometry (Model 700, Chrono-Log Corporation; Havertown, PA) [16]. Whole blood (500 μ L) was diluted 1:1 with 3mM CaCl₂ in 0.9% normal saline and incubated for 5 min at 37 °C. Platelet activators -- collagen (3.2 μ g/mL) or adenosine diphosphate (ADP) (2.5 μ g/mL) -- were added and the relative area under the curve (AUC), slope, and lag time were recorded for a 6-min test duration.

Platelet poor plasma was prepared by dual centrifugation (3,000 x g, 10 min) for assessment of coagulation using an STA Compact Max Coagulation Analyzer (Stago; Parsippany, NJ, USA). Prothrombin time (PT), activated partial thromboplastin time (aPTT), fibrinogen and D-dimer concentration, antithrombin III (ATIII) activity assay, and von Willebrand factor (vWF) antigen test were performed as previously reported [16].

2.5.4 Post-Circulation Circuit Thrombus Assessment

At the end of 6 h circulation, a 100 U heparin bolus was administered to all circuits to prevent additional clotting during circuit deconstruction. Tubing and pump heads were rinsed with phosphate buffered saline (PBS, pH=7.4) and inspected for deposition of macroscopic clots. The size and quantity of clots were recorded. A thrombus deposition scoring system was used (Table 2.3) to rank the severity of thrombus deposition from 0 (least severe, no visual thrombi) to 5 (most severe, thrombi impeding circuit flow/pump performance). Additionally, tubing samples were collected for SEM imaging as previously reported [17]. Samples were fixed with 2.5% glutaraldehyde in 0.1 M sodium cacodylate buffer for a minimum of 48 h, then dehydrated in graded ethanol (35%, 50%, 70%, 95%, 100%) and stored in a vacuum desiccator until SEM analysis. Samples were sputter-coated with gold at 20 nm thickness. Images were acquired at 500x magnification at an accelerating voltage of 5.00 kV.

2.5.5 Post-Circulation Tubing Activity Analysis

In addition to tubing SEM samples, tubing segments were collected for assessment of CuBTri catalytic activity following blood exposure. GSNO oxidation by CuBTri in the composite was used to evaluate the activity of the coatings before and after *ex vivo* studies. Prior to analysis, 1 cm segments of tubing were agitated in Millipore water overnight to remove residual blood residue, then air dried and placed in a custom reaction cell. Nitric Oxide Analyzers (280i, Zysense, Weddington, North Carolina) were used to track GSNO oxidation via chemiluminescence-based NO detection. Millipore water was added to the reaction cell for a final volume of 3 mL. After beginning the experiment, 10 μ M reduced glutathione and 25 μ M GSNO were sequentially injected into the reaction cell. The reaction proceeded at 25 °C shielded from light with constant nitrogen bubbling for 1 h with a collection interval of 1 s. Coatings were

determined to be active if total NO release was ≥ 5 times the baseline (10 μM reduced glutathione, 25 μM GSNO, 1 cm uncoated Tygon tubing) over equivalent reaction times. Activity below this threshold or $< \text{LOD}$ is inconclusive based on the current method due to sample size limitations and the inherent heterogeneity of the coatings.

2.6 Statistical Analysis

For coating stability tests, statistical differences were analyzed with a two-tailed t-test ($\alpha \leq 0.05$). For hemocompatibility statistical analyses (SAS 9.1; Cary, NC), all tests were two-sided with $\alpha \leq 0.05$ for significance. A Shapiro-Wilk test was conducted to test the distribution of data for normality. If skewed, the data were transformed, or the nonparametric version of the test was used. Groups were tested independently using a one-way mixed model with repeated measures and Dunnett adjustment to assess baseline changes. Group differences were examined using a two-way mixed model with repeated measures and a Tukey adjustment.

3. Results and Discussion

We aimed to engineer and evaluate a bioactive composite coating on medical-grade Tygon ND-100-65 (ID 3/8") tubing, comparable in size to commercial extracorporeal lung support systems (ex. Novalung XLUNG Kit 230, Xenios/Fresenius, Bad Homburg, Germany; and HLS Set Advanced 5.0/7.0, Getinge, Gothenburg, Sweden). The bioactive composite consists of Tygon doped with CuBTri, selected for its demonstrated ability to catalytically generate NO from RSNOs. On contact with blood, we hypothesized that localized NO generation from endogenous RSNOs would occur at the blood-surface interface to inhibit clotting. To this end, we fabricated a uniform coating, analyzed the stability under fluid flow, and assessed the activity of the CuBTri within the coating.

3.1 Bioactive MOF Composite Coating Fabrication

3.1.1 Exploratory Coating Procedures

A coating procedure was developed and optimized to uniformly coat the inner surface area of the extracorporeal circuit tubing. The CuBTTri is coated onto the Tygon tubing by pouring a coating solution containing Tygon polymer and CuBTTri across the inner surface area of the tubing. The dissolved Tygon acts as a bonding agent to adhere the CuBTTri onto the tubing, creating a polymeric composite coating. It is important that the CuBTTri particles are uniformly dispersed throughout the coating, so catalysis of NO occurs across the entire surface. If there is a cluster of settled MOF particles in one section of the tubing and a lack of particles in another, this could result in an inconsistent distribution of NO generation leading to localized clotting.

Originally, we used the coating procedure outlined by Zang et al. [13] where a coating solution with 1.0% w/v CuBTTri and 1.0% w/v Tygon polymer in THF was used to coat a seven-foot-long, 1/4" ID tubing. However, the procedure performed in this report uses a tubing diameter of 3/8", as that is the standard for ECMO. Therefore, we needed to increase the volume of the coating solution and it was more difficult to dispersedly coat the CuBTTri with the larger ID tubing.

Using Zang's initial procedure, Tygon polymer (0.6 g) was added to 30 mL of THF, which was stirred overnight to dissolve the polymer. The next day, CuBTTri (0.6 g) was added to 30 mL of THF which was sonicated (Branson, 3800 Ultrasonic Cleaner, Brookfield, CT) for 1 hour. The two solutions were combined and sonicated again for 1 hour. After the 2 hours of sonication, a portion of the CuBTTri particles remained settled. This is because sonication alone

did not permit the larger mass of CuBTTri to be suspended in this larger volume. Consequently, it was decided that two different coating solutions should be tested, one with 1.0% w/v CuBTTri and one with 0.1% w/v CuBTTri. Additionally, new solution preparation procedures were developed.

For both the 1.0% w/v and 0.1% w/v CuBTTri solutions, different iterations of the solution preparation were needed to perfect the process. Two of the major alterations from Zang's approach included hand grinding the CuBTTri for 10 minutes and the addition of a stirring step with sonication. Grinding and stirring allowed the CuBTTri particles to be fully suspended to establish a uniform coating solution. These two alterations are included in the following final coating solution procedure.

The Tygon solution was prepared by dissolving 0.60 g Tygon polymer in 30 mL THF and stirring overnight. The next day, either 0.6 g CuBTTri or 0.06 g CuBTTri (for the 1.0% w/v and 0.1% w/v solutions respectively) was added to 30 mL of THF. This solution was stirred rapidly for 20 min and sonicated for 30 min. The Tygon solution was added, and the entire solution was stirred for 20 min and sonicated for 30 min to fully suspend the CuBTTri in solution. This formed the coating solution which consisted of 1.0% w/v Tygon and either 1.0% w/v CuBTTri or 0.1% w/v CuBTTri.

After the coating solution was developed, a modified coating procedure was used to uniformly coat the 3/8" ID Tygon extracorporeal circulation tubing. The initial procedure to coat the tubing originally performed by Zang is shown in Figure 2.4. The Tygon tubing was connected on one end to a 22" segment of 3/8" ID pump tubing (Pumpsil #36, Falmouth, United Kingdom) which was inserted through the peristaltic pump (Watson Marlow, 9131, Falmouth, United Kingdom). The Tygon tubing laid flat on the ground with one end in the coating

solution. The peristaltic pump was turned on to 165.4 RPM (2.5 L/min) so the coating solution could flow through the tubing, coating it with CuBTri. With the larger ID tubing, the coating solution flowed at a slower rate, and did not fill the entire diameter of the tubing. This resulted in the settling of CuBTri particles along the bottom side of the tubing as shown in Figure 2.5, thus further adaptations were needed to uniformly coat the tubing.

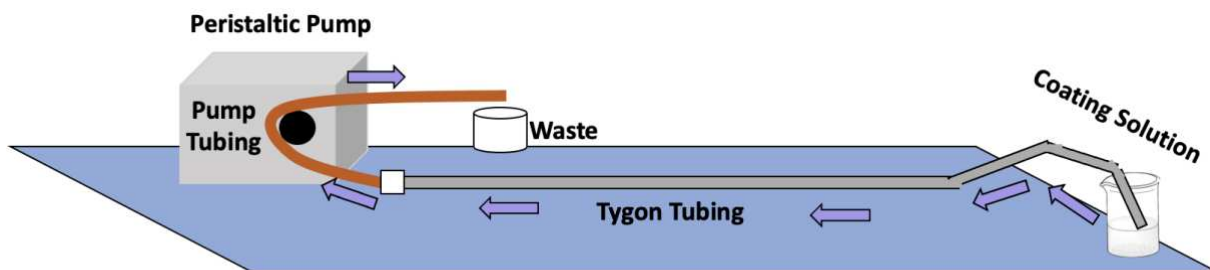


Figure 2.4. First iteration of the CuBTri coating procedure.



Figure 2.5. Image of settled CuBTri on the tubing that was coated with the initial coating procedure using 0.1% w/v CuBTri.

To address these issues, we modified the method in three important ways. First, we increased the flow rate of the pump to 175 RPM (2.646 L/min), though this was not sufficient to evenly coat the tubing. Second, we angled the tubing to flow downward toward the pump by

elevating the far end of the tubing 8” from the ground, shown in Figure 2.6a. The coating solution was then poured into the tubing instead of being sucked through. This modification increased the flow rate of the coating solution, which helped inhibit some CuBTTri settling, as there was less time for the particles to clump together; but the solution did not fill the entire diameter of the tubing as required to coat the entire surface area because the solution did not come into contact with the top half of the tubing. Third, we attached a 22” segment of 1/2" ID tubing (Fisher, 14-169-7J, Hampton, NH) to the elevated end of the tubing with a clamp, as shown in Figure 2.6b. After the 60 mL coating solution was poured into the 1/2” ID tubing, the clamp was released, and the peristaltic pump was turned on to 175 rpm (2.646 L/min). This created a bottleneck effect that allowed the coating solution to completely fill the diameter of the tubing and flow uniformly through the length of the tubing. This iteration displayed promise as the 0.1% w/v formulation showed no visual signs of CuBTTri settling, as seen in Figures 2.7a and 2.7b. Additionally, the SEM image in Figure 2.7c verified the even dispersion of the CuBTTri particles throughout the tubing. The 1.0% w/v formulation still displayed a streak of settled CuBTTri particles as seen in Figures 2.8a and 2.8b. Similarly, the SEM image in Figure 2.8c for the 1.0% w/v formulation displayed slight agglomeration of CuBTTri particles. These findings indicate that the 0.1% w/v would be preferred given uniformity of this coating increases the likelihood of consistent NO generation across the surface area of the tubing, better resembling the endothelium. However, both formulations were used in future experiments to further compare.

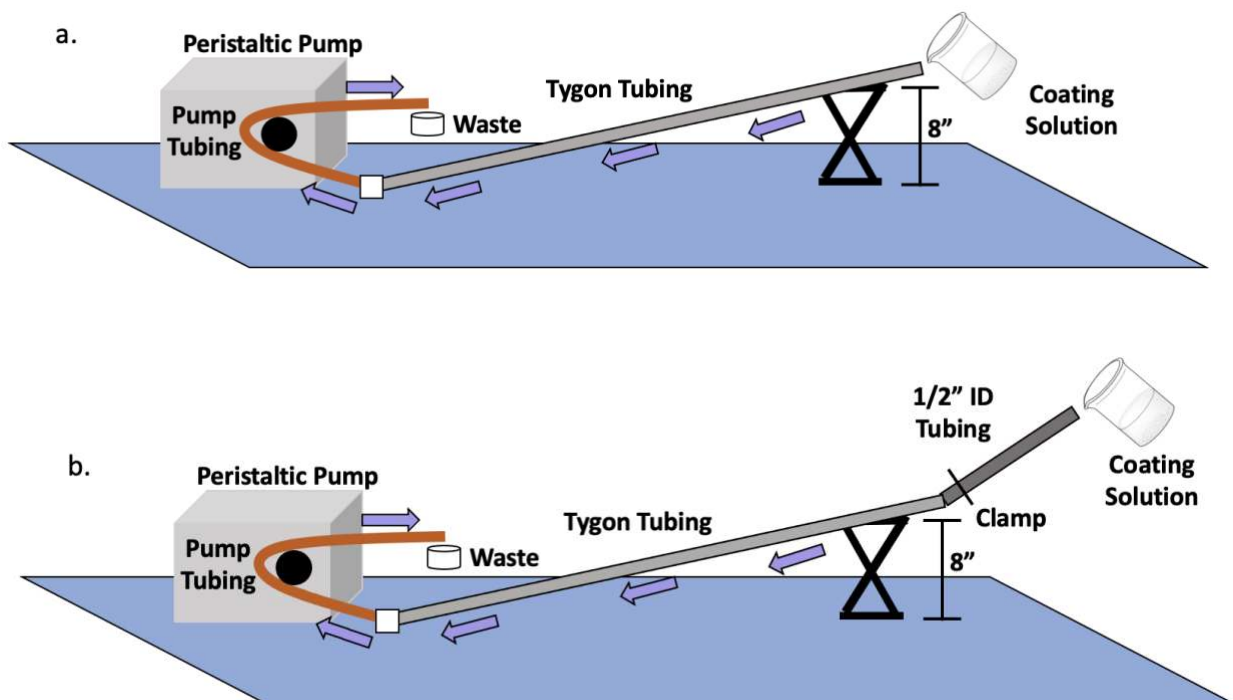


Figure 2.6. (a) The second iteration of the coating procedure. The coating solution was poured into the elevated tubing to increase the flow rate. This helped evenly disperse the CuBTtri particles, but the entire inner surface area of the tubing was not coated. (b) The third and final iteration of the coating procedure. A 1/2" ID tubing was added to hold the solution, creating a bottleneck effect so the entire inner surface area of the tubing was coated with dispersed CuBTtri.



Figure 2.7. (a, b) Tubing coated with the final iteration procedure using 0.1% w/v CuBTtri. There are no signs of agglomeration or settling of the CuBTtri particles. (c) SEM image of the dispersed CuBTtri particles on the tubing, further confirming there is no agglomeration. SEM image was taken using 15.0 kV at 100x magnification.



Figure 2.8. (a, b) Tubing coated with the final iteration procedure using 1.0% w/v CuBTtri. The tubing is purple from the purple CuBTtri particles and there is a streak of obvious settling in image (b). (c) SEM image of the CuBTtri particles on the tubing, some agglomeration might be present. SEM image was taken using 15.0 kV at 100x magnification.

3.1.2 Solvent Removal

After the coating procedure, it is essential to remove the THF from the coating to not endanger the patient, given the toxicity of the solvent. The tubing was put under vacuum in 60°C and analyzed with GC periodically until THF was no longer detected (<DL). Using this analysis,

it was determined that leaving the tubing in this environment for approximately 2 weeks was sufficient to remove any residual THF in the coating.

3.2 Tubing Activity Analysis

After the solvent was removed, the tubing was analyzed for NO release in the presence of an endogenous NO donor, *S*-nitrosoglutathione (GSNO). The NO fluxes are 0.00032 ± 0.00029 nmol/min/cm², 0.05 ± 0.02 nmol/min/cm², and 0.05 ± 0.03 nmol/min/cm² for the uncoated tubing (control), 0.1% w/v formulation, and 1.0% w/v formulation respectively, as seen in Figure 2.9. There is a significant increase in NO release when comparing either CuBTTri formulation to the control ($p < 0.05$), but there is no significant difference between the generation of NO for each of these formulations ($p > 0.05$). Additionally, the total NO generation is $3.92 \times 10^{-11} \pm 1.60 \times 10^{-11}$ nmol, 57 ± 1 nmol, and 54 ± 2 nmol for the control, 0.1% w/v formulation, and 1.0% w/v formulation respectively as seen in Figure 2.10. This infers that for the same amount of NO donor, about the same amount of NO is generated from the coating ($p > 0.05$). Therefore, it can be concluded that catalysis occurs at about the same rate for each of the formulations. Initially, I hypothesized that a higher concentration of CuBTTri would catalyze NO generation faster, but this is not the case. It is now hypothesized that only a fraction of the cationic nodes from the CuBTTri are available on the surface of the coating. Because GSNO is a large molecule with a molecular weight of 336.32 g/mol, it cannot penetrate the Tygon coating and NO catalysis only occurs on the surface. Therefore, even though there is more CuBTTri on the 1.0% w/v formulation tubing, the GSNO can only reach the catalysts on the surface. The small differences in the generation of NO allow the option to choose either formulation for the project, but given the initial results from the coating procedure, the 0.1% w/v formulation is preferred.

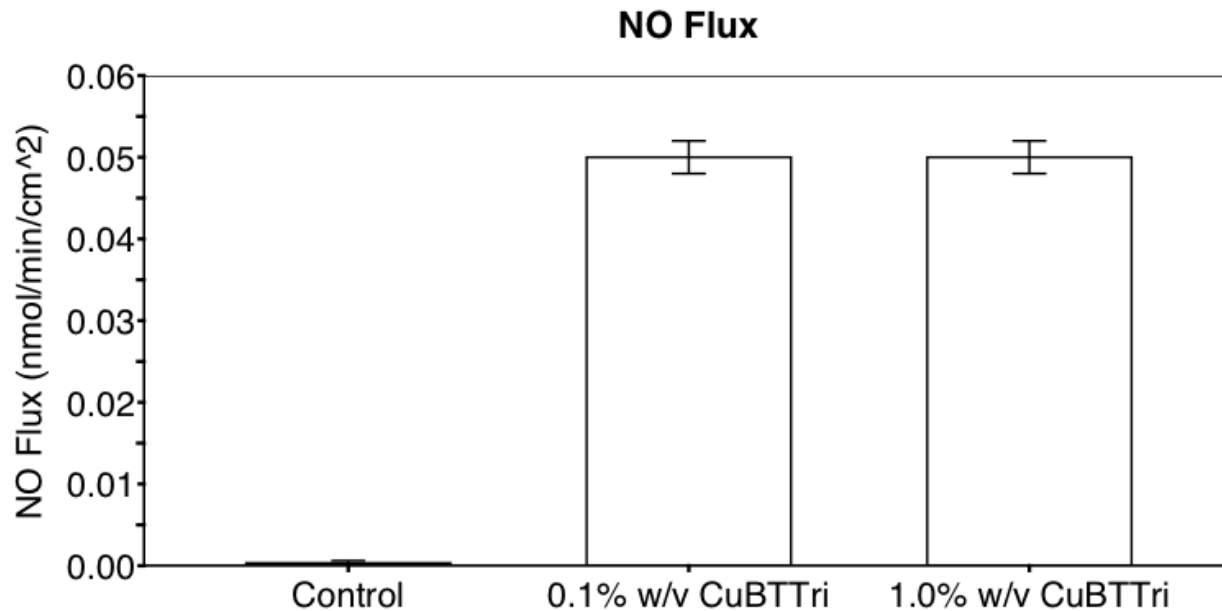


Figure 2.9. NO flux for each of the different CuBTtri formulations compared to a control. There is no statistical difference between the 0.1% w/v CuBTtri and 1.0% w/v CuBTtri.

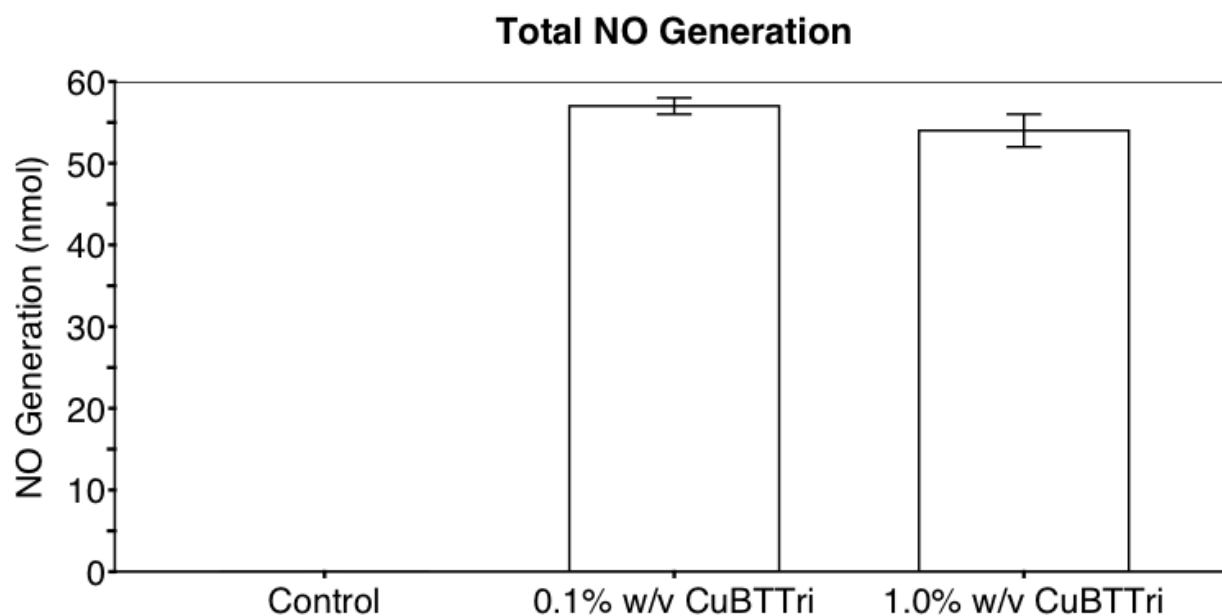


Figure 2.10. Total NO generation for each of the different CuBTtri formulations compared to a control. There is no statistical difference between the 0.1% w/v CuBTtri and 1.0% w/v CuBTtri.

3.3 Evaluation of Coating Stability Under Flow Conditions

3.3.1 Delamination Testing

One of the concerns in developing a composite coating with a copper-based MOF is the potential for coating delamination or MOF degradation due to fluid flow, as this could endanger the patient receiving extracorporeal organ support [18]. 24 h saline flow circuits (see Figure 2.2) were used to determine the stability of the coating using clinical fluid flow rates for partial lung support (1.5 L/min – 2.5 L/min) [19]. The morphology of the coating was visualized with SEM before saline circulation and after the 24-h circuit. Figure 2.11(a-f) display SEM images using the 0.1% CuBTTri formulation taken before the 24-h circuits (Figure 2.11(a-c)) and after the 24-h circuits (Figure 2.11(d-f)). Additionally, Figure 2.12(a-f) display SEM images using the 1.0% CuBTTri formulation taken before the 24-h circuits (Figure 2.12(a-c)) and after the 24-h circuits (Figure 2.12(d-f)). With both of these formulations, there were no signs of visual coating delamination, as the CuBTTri particles remained on the tubing surface and the coating itself remained intact. It is important to note the images taken before and after the 24-h circuit are different pieces of tubing, so it is expected that the images do not look exactly the same.

72-h saline circuits were used to determine if delamination was occurring after a prolonged period. For the first 24 h, saline flowed at 1.5 L/min and increased to 2.0 L/min after 24 h and 2.5 L/min after 48 h. This was to determine if there was a specific flow rate that delaminated the coating. Figure 2.13 and Figure 2.14 displays SEM images using the 0.1% CuBTTri and 1.0% CuBTTri formulations respectively at each 24 h interval. Again, there was no signs of visible delamination allowing us to conclude that the coating stays in-tact for up to 72-h using standard ECMO flow rates.

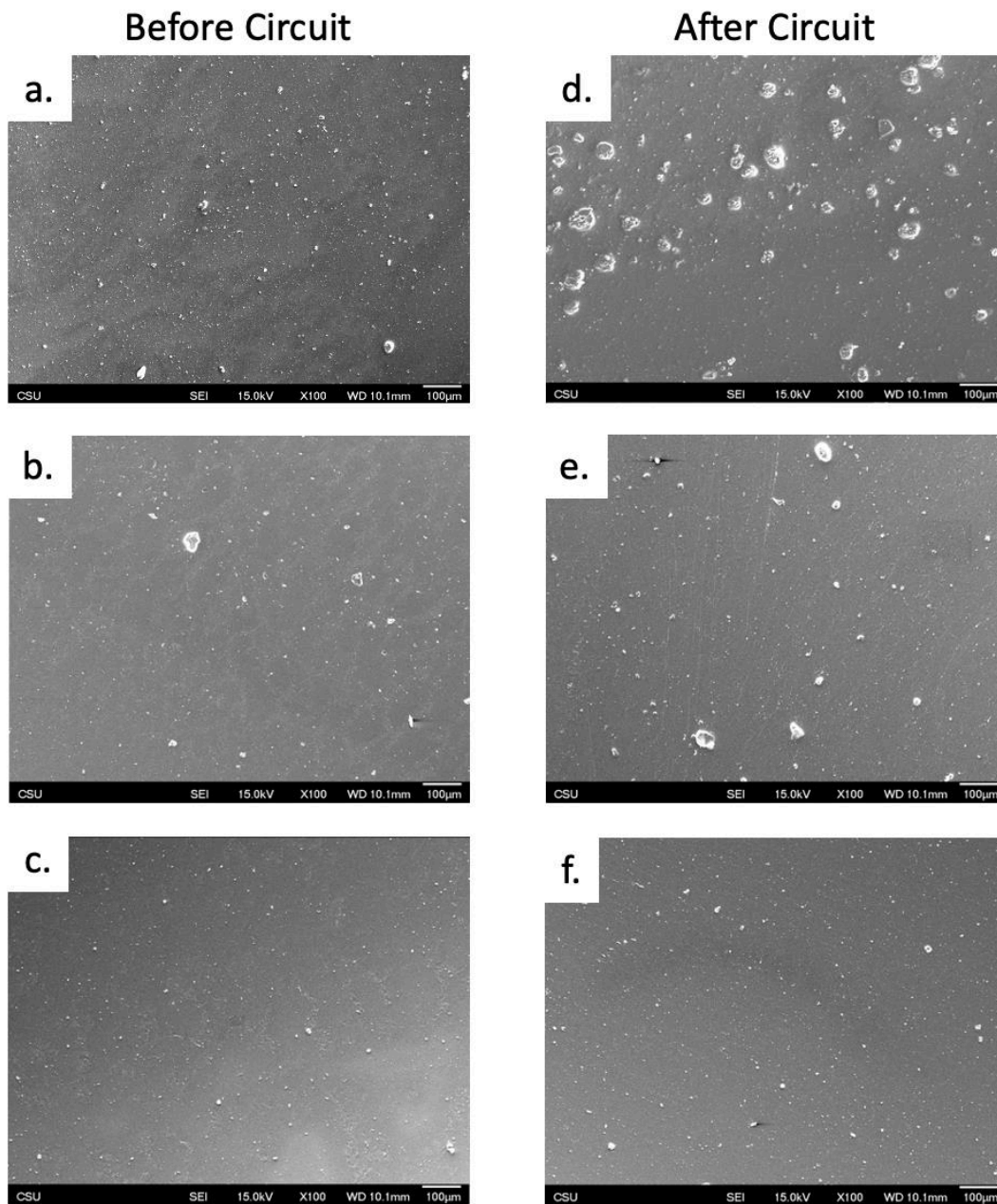


Figure 2.11. Three samples of the 0.1% w/v formulation on tubing before and after a 24-hour saline flow loop experiment. Figures on left (a-c) correspond to tubing before the flow loop and figures on the right (d-f) correspond to tubing after 24 hours of flow at 2.5 L/min. There is no apparent delamination occurring after 24 hours of saline flow. SEM images were taken using 15.0 kV at 100x magnification.

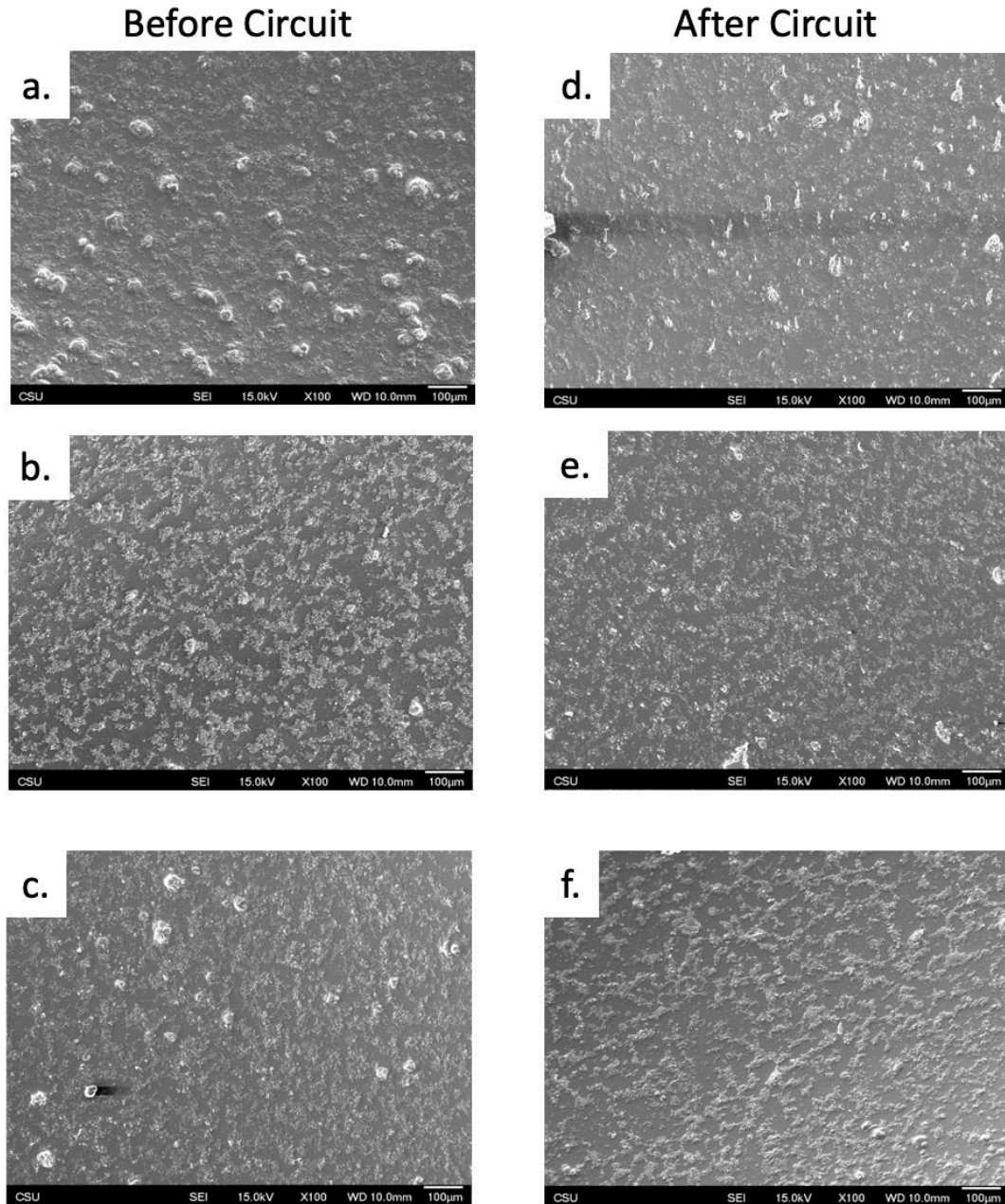


Figure 2.12. Three samples of the 1.0% w/v formulation on tubing before and after a 24-hour saline flow loop experiment. Figures on left (a-c) correspond to tubing before the flow loop and figures on the right (d-f) correspond to tubing after 24 hours of flow at 2.5 L/min. There is no apparent delamination occurring after 24 hours of saline flow. SEM images were taken using 15.0 kV at 100x magnification.

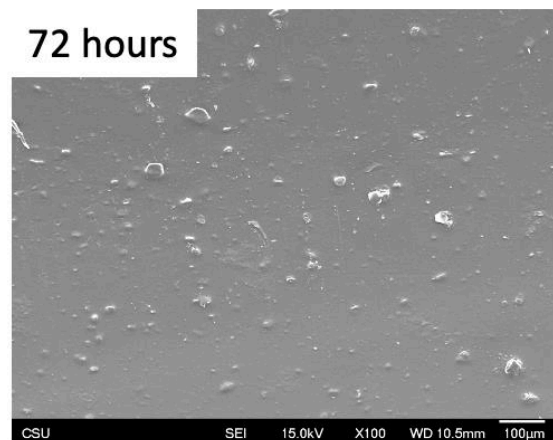
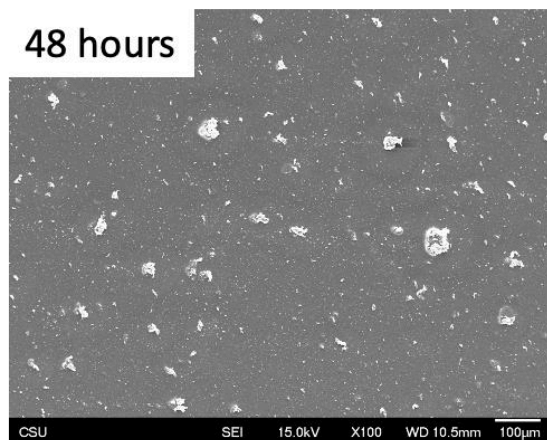
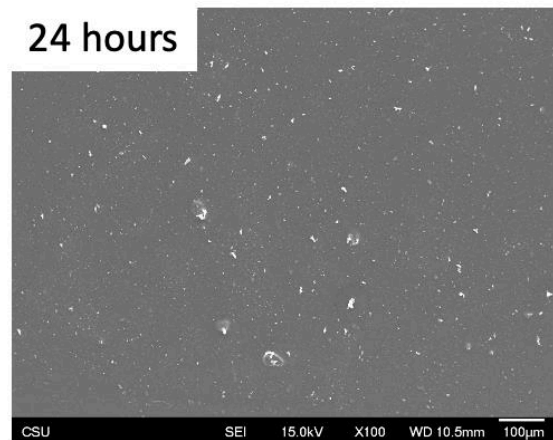
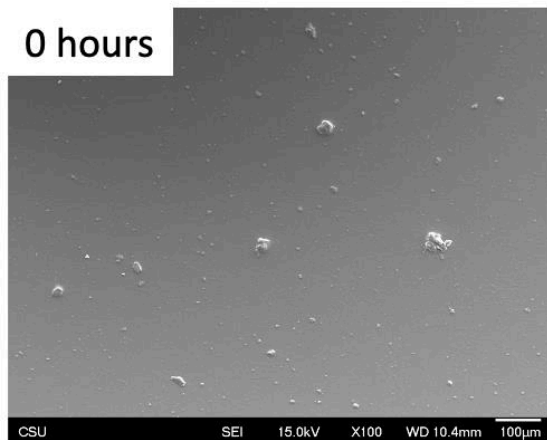


Figure 2.13. SEM images of the tubing coated with the 0.1% w/v CuBTtri formulation at each time point during the 72-h saline circuit. There is no apparent delamination occurring at each time point. SEM images were taken using 15.0 kV at 100x magnification.

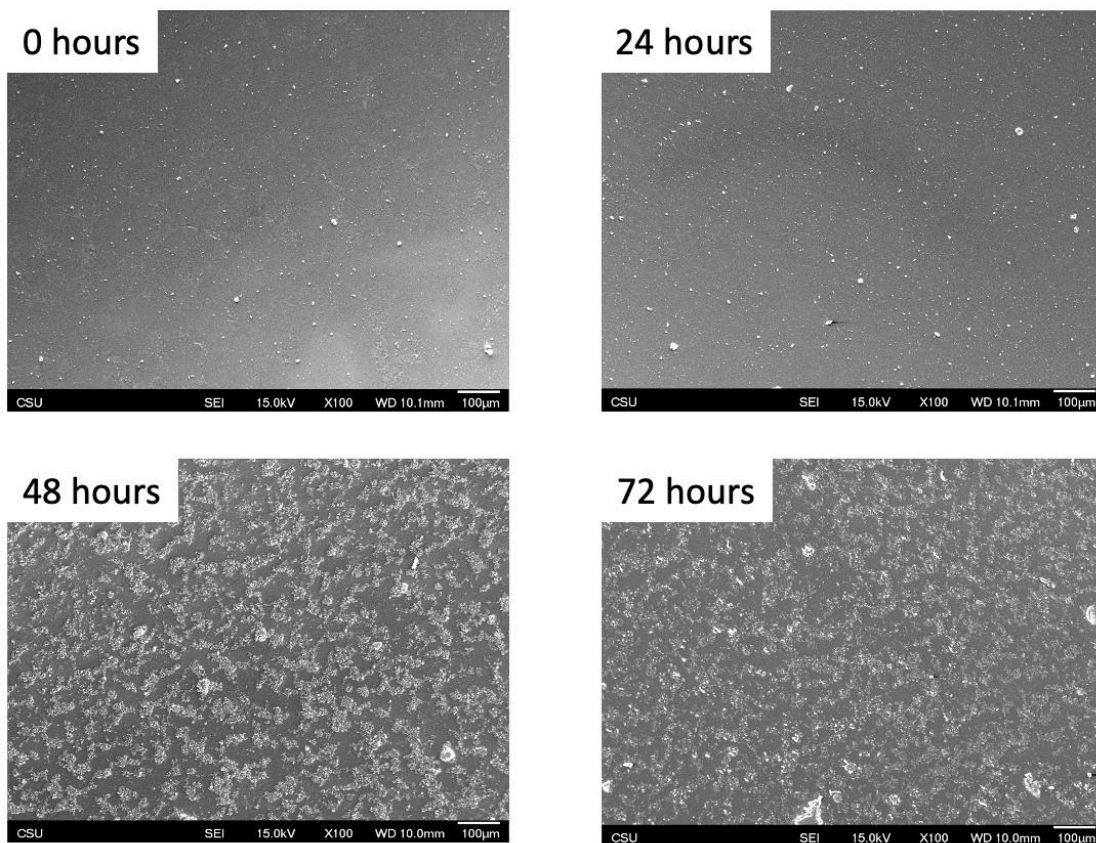


Figure 2.14. SEM images of the tubing coated with the 1.0% w/v CuBTTri formulation at each time point during the 72-h saline circuit. There is no apparent delamination occurring at each time point. SEM images were taken using 15.0 kV at 100x magnification.

3.3.2 MOF Stability

It was previously reported that many copper-based MOFs, which are not stable under physiological conditions, degrade into copper ions and their associated ligand when exposed to water [18]. CuBTTri has previously been shown to be stable in water, but has yet to be evaluated under dynamic flow conditions [11], [12]. To determine if the MOF was degrading due to fluid flow, we measured the copper concentration of the circulated saline solution at each 24 h interval

for both the 24 h and 72 h experiments (24 h or 24 h, 48 h, and 72 h) and compared them to a control solution (0 h).

Results for the 24-h flow circuit are displayed in Figure 2.15. Using the 0.1% w/v formulation, the copper concentration before and after 24 h circuit was 10.7 ± 4.5 ng/mL and 8.3 ± 2.1 ng/mL respectively. Using the 1.0% w/v formulation, the copper concentration before and after 24 h circuit was 7.3 ± 4.5 ng/mL and 18.7 ± 3.4 ng/mL respectively. These results indicated that the 0.1% w/v formulation did not cause any degradation of the MOF, as there was no increase in copper concentration after 24 h of flow ($p > 0.05$). However, even though there was not a statistically significant change in the copper concentration for the 1.0% w/v formulation ($p > 0.05$), there was still a large increase in copper concentration. There are a couple of explanations for this increase in copper: 1) the MOF is degrading and leaching copper into the system or 2) unbound copper ions that were left over from the synthesis are exposed. It is important to determine which is occurring, because if CuBTTri is degrading, this could affect the safety of the coating. Future experiments are needed to determine if CuBTTri is stable; one option is to use time-of-flight mass spectrometry to confirm the presence of the ligand, H₃BTTri in the saline solution. If H₃BTTri is present, this would indicate that the MOF is degrading.

Results for the 72-h flow circuit are displayed in Figure 2.16. Using the 0.1% formulation, the copper concentrations at 0 h, 24 h, 48 h, and 72 h were 5.3 ± 1.2 ng/mL, 8.7 ± 1.2 ng/mL, 16.5 ± 10.5 ng/mL, and 12.7 ± 3.3 ng/mL respectively. Using the 1.0% formulation, the copper concentrations at 0 h, 24 h, 48 h, and 72 h were 11.0 ± 0.65 ng/mL, 10.6 ± 0.28 ng/mL, 11.0 ± 0.37 ng/mL, and 11.7 ± 0.82 ng/mL respectively. For both of these formulations, there was no statistical difference in copper concentration at any of the time points as compared to their respective control (0 h) ($p > 0.05$). However, it is worth to note the large increase in the

0.1% w/v formulation at the 48-h mark, as there was an outlier which significantly skewed the results, and it seems as if the copper concentration increases with time during the 72 h flow. Similarly to the explanation above, I hypothesize this increase could be from the CuBTri degrading, or unbound copper ions left over from the synthesis are exposed due to fluid flow. If the MOF is not degrading, I believe the coating can be used safely as there are only nanograms of copper being leached. Comparing the study performed by Major et al., this application leaches much less copper (approximately 1,000x less) and it is and drastically under the recommended daily limit, which is 900 $\mu\text{g}/\text{day}$ [20]. Using these results, I still believe 0.1% w/v formulation is superior, but added experimentation will be required to ensure the coatings safety.

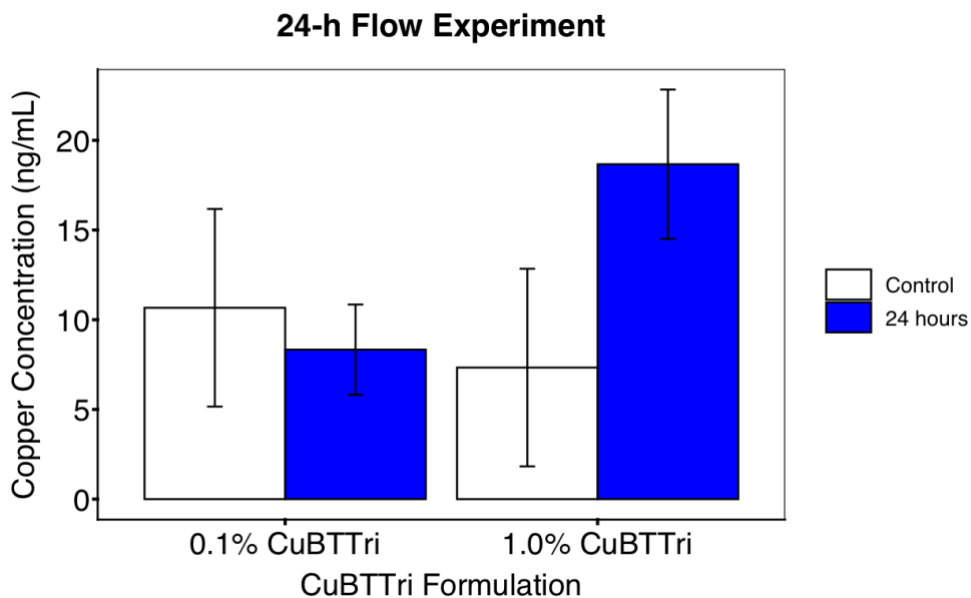


Figure 2.15. Copper concentrations of the saline before (white) and after (blue) the 24-h flow circuit. There were no statistical differences for either CuBTri formulation when compared to the control, but the difference appears larger with the 1.0% CuBTri formulation, possibly indicating that MOF degradation is occurring.

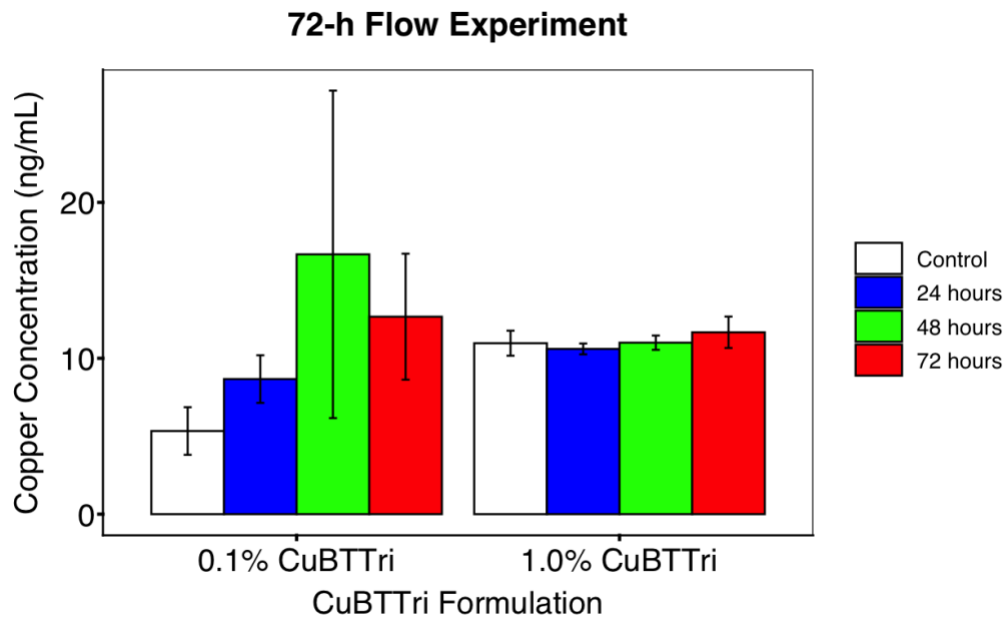


Figure 2.16. Copper concentrations of the saline at each time point during the 72-h flow circuit. There were no statistical differences for either CuBTtri formulation at any of the time points when compared to the control.

3.4 *Ex Vivo* Blood Compatibility Testing (6 h) under Clinical Flow Conditions

The ultimate aim of the coating is to avoid disrupting blood function. New technologies should have reversible effects on platelets without any other systemic influences. For example, the technology should limit blood clotting at the artificial surface without inducing systemic anticoagulation that may cause internal bleeding or other hemorrhagic complications to the patient. This means that upon removal from the coating surface, the blood should coagulate normally. The coated tubing segments were sent to members within the Autonomous Reanimation and Evacuation Research Program in San Antonio, TX, USA to perform *ex vivo*

circulation studies. This section contains a summary of their results to indicate the hemocompatibility of the coating.

To examine the viability of blood exposed to CuBTri coated Tygon tubing during *ex vivo* circulation, the following was assessed: 1) stability of circuit conditions during blood circulation (circuit patency, blood pump stability, anticoagulation requirements); 2) stability of blood during circulation (cell count and blood chemistry); 3) preservation of blood function during circulation (activity and aggregation of platelets, tests of blood coagulation); and 4) extent of clot deposition on the blood-contacting surface following 6 h blood exposure. Importantly, we used blood from donors that encountered polytrauma injury to simulate the abnormal coagulation status of sick patients that receive extracorporeal organ support. Therefore, we did not anticipate that blood cell counts and coagulation outcomes of circulated blood would be within the range of healthy, normal subjects. Rather, we focused on stability of blood cell counts and coagulation indices from start of blood circulation to end of circulation, anticipating that if the CuBTri coating was compatible with blood we would not observe dramatic fluctuations in markers of blood health over time.

3.4.1 Circuit Stability: Patency, Pump Performance and Anticoagulation

All circuits remained patent for the 6-h duration of the study; and the pump revolutions per min required to maintain the flow rate were similar and unchanging in both groups as displayed in Table 2.1. This suggests that no large clots were formed on the artificial surfaces causing an obstruction to blood flow. Small volumes of heparin anticoagulation were administered during circulation to maintain a physiologically relevant activated clotting time (ACT). Blood in both groups was consistently maintained in the target ACT range of 125-160 s.

There was a non-significant trend towards a higher heparin requirement to maintain the ACT target in the CTRL group than in the CuBTTri group (~25% increase; $p > 0.05$).

Table 2.1. Hourly hemocompatibility circuit results for unmodified Tygon tubing (CTRL, n=8) versus Tygon with 0.1% w/v CuBTTri coating applied (CuBTTri, n=8). Mean \pm standard error of activated clotting time (ACT), total heparin administered to achieve target ACT, and blood pump revolutions per min (RPM) to maintain the goal blood flow rate of 1.5 L/min. **Indicates significant change from baseline (BL) in CTRL. *Indicates significant change from BL in CuBTTri Group. All tests were two-sided tests with $p < 0.05$ for significance.

	Group	BL	1H	2H	3H	4H	5H	6H
ACT (sec)	CTRL	152 \pm 6	143 \pm 2	147 \pm 5	139 \pm 4**	136 \pm 3**	134 \pm 4**	136 \pm 3**
	CuBTTri	148 \pm 5	144 \pm 4	145 \pm 2	141 \pm 4	137 \pm 3*	131 \pm 3*	137 \pm 2
Heparin (U)	CTRL	3 \pm 3	56 \pm 33	78 \pm 46	81 \pm 45	99 \pm 44	109 \pm 46	118 \pm 50
	CuBTTri	6 \pm 4	44 \pm 24	60 \pm 31	60 \pm 31	72 \pm 35	84 \pm 32	88 \pm 34
Pump RPM	CTRL	1810 \pm 30	1810 \pm 30	1830 \pm 30	1810 \pm 30	1830 \pm 30	1810 \pm 30	1810 \pm 30
	CuBTTri	1810 \pm 40	1810 \pm 30	1830 \pm 30	1810 \pm 30	1830 \pm 30	1810 \pm 30	1800 \pm 30

3.4.2 Blood Stability: Cell Count and Chemistry

We did not observe any difference in blood cell counts, hemoglobin concentration or hematocrit between groups during the 6-h study as displayed in Table 2.2. White blood cell (WBC) count was statistically reduced in both groups beginning at 3 h; however, clinically this difference was minimal. No group differences in WBC differential were observed. Because the decrease in WBC count was highly similar and consistent between the CuBTTri and CTRL group, we anticipate that these effects were a result of the *ex vivo* blood circulation and were not attributed to the CuBTTri coating surface.

Table 2.2. Mean \pm standard error of complete blood cell count (WBC = white blood cell; RBC = red blood cell), hemoglobin, and hematocrit outcomes for unmodified Tygon tubing (CTRL, n=8) versus Tygon with 0.1% w/v CuBTTri coating applied (CuBTTri, n=8). **Indicates significant change from baseline (BL) in CTRL. *Indicates significant change from BL in CuBTTri Group. All tests were two-sided tests with $p < 0.05$ for significance.

	Group	BL	3H	6H
WBC ($\times 10^3/\mu\text{L}$)	CTRL	12 \pm 1	11 \pm 1**	11 \pm 1**
	CuBTTri	12 \pm 1	11 \pm 1*	11 \pm 1*
RBC ($\times 10^6/\mu\text{L}$)	CTRL	4.5 \pm 0.3	4.5 \pm 0.2	4.5 \pm 0.3
	CuBTTri	4.6 \pm 0.3	4.5 \pm 0.3	4.5 \pm 0.3
Hemoglobin (g/dL)	CTRL	8.1 \pm 0.5	8.1 \pm 0.5	8.1 \pm 0.5
	CuBTTri	8.1 \pm 0.5	8.1 \pm 0.5	8.1 \pm 0.5
Hematocrit (%)	CTRL	24 \pm 1	25 \pm 1	25 \pm 1
	CuBTTri	24 \pm 1	25 \pm 1	25 \pm 1

3.4.3 Blood Function: Platelet Activity and Tests of Coagulation

Group differences in platelet count and degree of platelet activation were of particular interest in this study, as CuBTTri has been shown to enhance NO release from endogenous donor species in the blood; and thus, may have the potential to reduce platelet activation, aggregation and subsequent platelet consumption [21]. We did not observe a difference in platelet count between groups over time, and loss of platelets in both groups was clinically minimal as seen in Figure 2.17. Additionally, the concentrations of activated (P-selectin-expressing) and procoagulant (phosphatidyl serine-expressing) platelets were not different between groups as seen in Figures 2.17b and c; although in both groups an increase in procoagulant platelets was observed by 6 h.

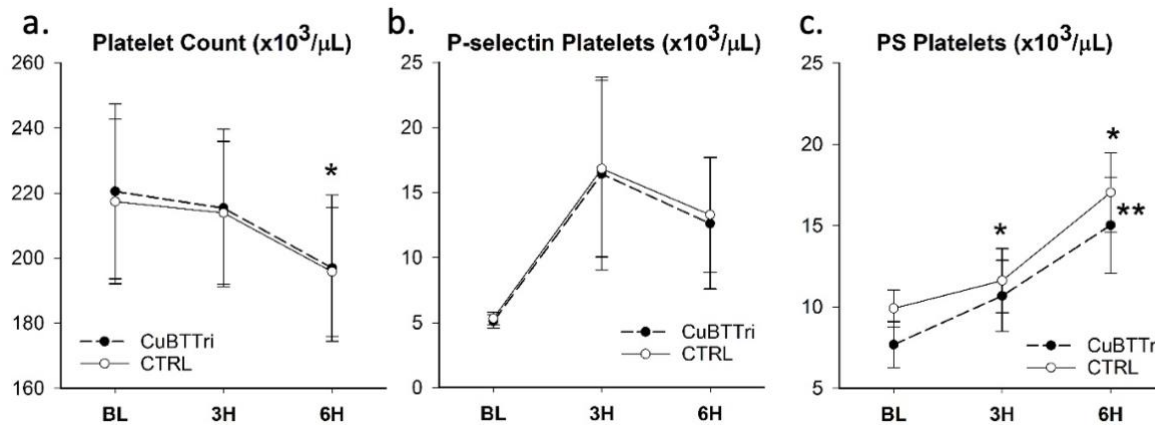


Figure 2.17. Platelet count (a) and degree of activated platelets (P-selectin platelets, b) and procoagulant platelets (phosphatidyl serine [PS] platelets, c) in blood circulated *ex vivo* through Tygon tubing (CTRL, n=8) versus Tygon with 0.1% w/v CuBTTRI coating applied (CuBTTRI, n=8). Results expressed as mean \pm standard error. **Indicates significant change from baseline (BL) in CTRL. *Indicates significant change from BL in CuBTTRI Group. All tests were two-sided tests with $p < 0.05$ for significance.

Similar to platelet activation results, we observed no difference in coagulation test results between the groups and shown in Figure 2.18. Thromboelastography reaction time, which measures the time to start of clot detection in whole blood, was significantly shortened in both groups by 6 h compared to baseline. This means that circulating blood developed a propensity to clot more rapidly over time during the 6-h circulation. Because this trend occurred similarly in both groups, we anticipate that this was an effect of blood exposure to shear stress and foreign surfaces in the *ex vivo* circuit and was not an untoward effect of the CuBTTRI coating. Additionally, there was not an observed difference between the groups in clot formation time and clot strength in 6 h. Cumulatively, coagulation tests suggested a trend towards more rapid initiation of thrombus formation in both groups over the course of the 6-h study; however no

between-group differences were observed, again suggesting no untoward effects of CuBTri on blood activity.

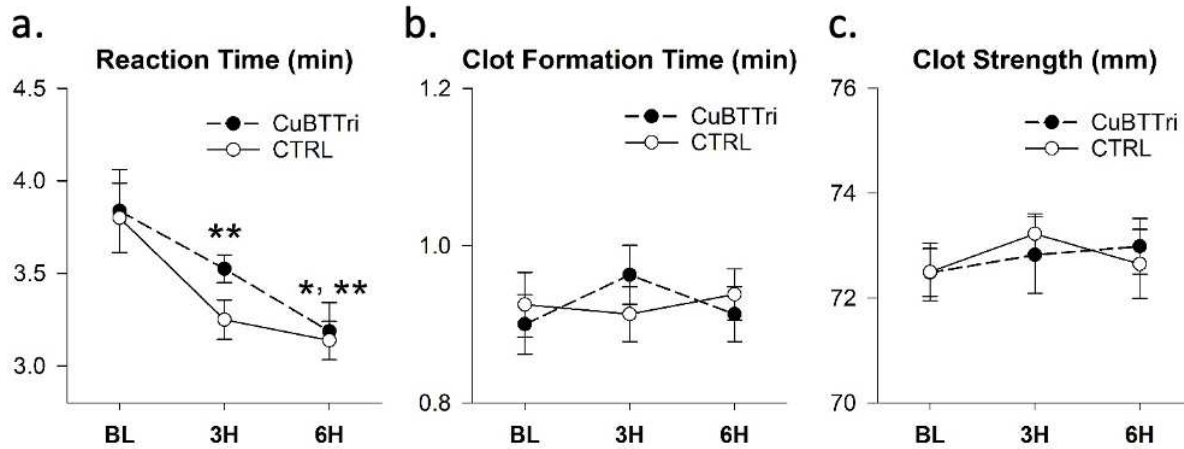


Figure 2.18. Reaction time, clot formation time, and clot strength in blood circulated *ex vivo* through Tygon tubing (CTRL, n=8) versus Tygon with 0.1% w/v CuBTri coating applied (CuBTri, n=8). Results expressed as mean \pm standard error. **Indicates significant change from baseline (BL) in CTRL. *Indicates significant change from BL in CuBTri Group. All tests were two-sided tests with $p < 0.05$ for significance.

The potential of CuBTri to enhance NO production, and subsequently reduce platelet activation and aggregation, is dependent on availability of endogenous NO-donor species such as RSNOs. However, the concentration of NO-donor species in the injured swine donor blood during this 6-h experiment is unknown, due to measurement limitations [22]. Furthermore, synthesis and metabolism of NO donor species cannot be fully replicated in an *ex vivo* setting outside the vascular endothelium [23], which is a limitation of this study. This limitation could explain why no significant anticoagulant benefit was observed to differentiate the CuBTri tubing versus unmodified Tygon in this study. The finding that CuBTri does not disturb blood

function during circulation is a positive outcome of this *ex vivo* study. Further *in vivo* testing is required to accurately assess the antithrombogenic properties of this technology.

Others have investigated the utility of NO-catalyzing surface coatings similar to CuBTTri while supplying an exogenous source of RSNOs to enhance NO production [20], [24]. Douglass and colleagues demonstrated that a multilayer coating with incorporated Cu nanoparticles and *S*-nitrosoglutathione (GSNO) preserved platelet count and reduced macroscopic thrombus deposition on Tygon tubing in a 4-h rabbit arteriovenous shunt model; of note, these benefits were not observed when a single-layer Cu-nanoparticle coating was utilized without the GSNO layer [24]. Likewise, Major et al investigated a Cu-nanoparticle-containing polyurethane material utilized with continuous infusion of an exogenous RSNO, *S*-nitroso-*N*-acetylpenicillamine, in a 4-h rabbit arteriovenous shunt model. They also reported that the combination of both Cu coating and exogenous RSNO was required to observe preservation of platelet count and a reduction in macroscopic thrombus development compared to control [20]. Thus, it is possible that introduction of RSNOs from an exogenous source in combination with the CuBTTri coating may have led to improved antithrombogenic outcomes in the present study. However, in this initial development and characterization study we sought to investigate the safety and efficacy of this approach without introducing RSNOs from exogenous sources.

3.4.4 Post-Circulation Thrombus Deposition

Tubing and blood pump surfaces were inspected following 6 h blood exposure to assess degree of thrombus deposition. A clot deposition score (0-5, see Table 2.3) was used to report the extent of macroscopic clot deposition, and SEM imaging was used to assess quality of thrombi. Overall, the mean thrombus deposition scores indicated minimal clotting with no

difference between CTRL tubing (1.5 ± 0.4) and CuBTTri tubing (1.9 ± 0.4). Likewise, mean thrombus deposition scores for the blood pumps were not different between CTRL (1.6 ± 0.3) and CuBTTri (1.3 ± 0.2). SEM imaging of post-circulation tubing revealed minimal thrombus deposition and was highly comparable between groups as seen in Figure 2.19. CuBTTri was visualized on the tubing surface.

Table 2.3. Post-circulation tubing and pump thrombus deposition scoring system. Note, for measurement of thrombus size the size limits apply to clot dimension in any direction (length, width, height). Each clot size was classified by the longest dimension.

Thrombus Score	Pump	Tubing
0	no thrombi visualized	no thrombi visualized
1	thrombus size ≤ 1 cm and ≤ 3 thrombi visualized in total	thrombus size ≤ 1 cm and ≤ 3 thrombi visualized in total
2	thrombus size > 1 cm but ≤ 3 cm and/or > 3 but ≤ 10 distinct thrombi visualized	thrombus size > 1 cm but ≤ 3 cm and/or > 3 but ≤ 10 distinct thrombi visualized
3	thrombus size > 3 cm but ≤ 10 cm and/or > 10 distinct thrombi	thrombus size > 3 cm but ≤ 10 cm and/or > 10 distinct thrombi
4	thrombus size > 10 cm and/or pump RPMs significantly elevated (relative to baseline) with thrombus visualized post-circulation	thrombus size > 10 cm and/or thrombus reducing tubing inner lumen by 10-25%
5	thrombus causing pump occlusion/failure	thrombus reducing tubing lumen by $> 25\%$ Or Thrombus causing tubing occlusion

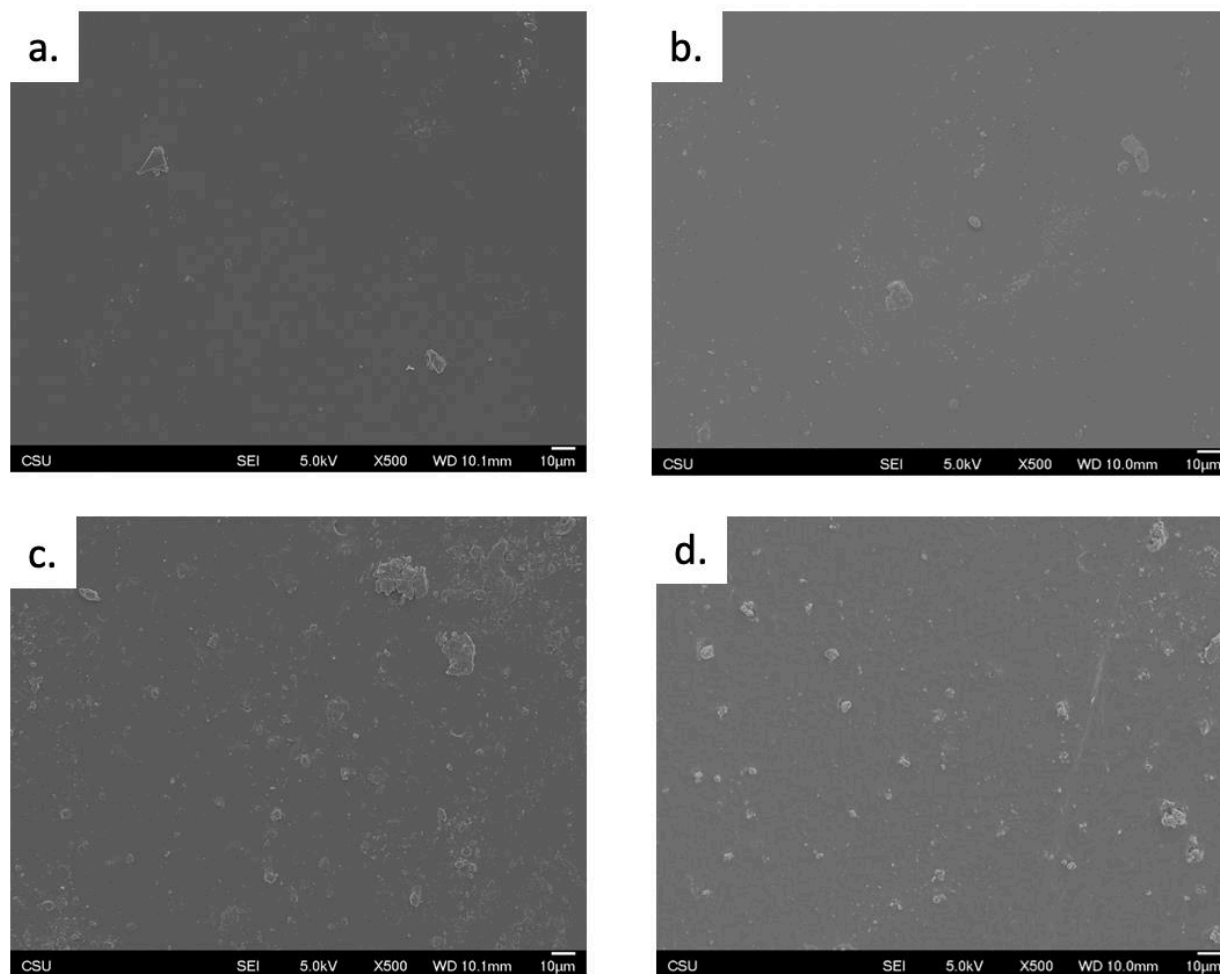


Figure 2.19. Representative scanning electron microscopy images (500x magnification) of tubing following 6 h blood circulation *ex vivo* through Tygon tubing with 0.1% w/v CuBTTRi coating applied (CuBTTRi; a, b) versus unmodified PVC (CTRL; c, d).

3.4.5 Limitations

Limitations of the blood hemocompatibility study include the use of swine donor blood and interspecies variability. Swine blood is recommended as a human blood alternative during testing of coagulation for extracorporeal organ support devices to mimic clinical conditions and coagulation parameters [25]; however, species differences in endogenous RSNO levels and

effects of polytrauma on swine RSNO levels may limit clinical translation. Additionally, the *ex vivo* nature of the hemocompatibility test requires administration of systemic anticoagulation and limits the duration of testing due to blood viability. We attempted to minimize the impact of systemic anticoagulation by sparingly utilizing heparin to an ACT target (125-160 s) that is lower than levels clinically utilized in patients received extracorporeal lung support (180-200+ s) [26]. However, use of heparin and the short experiment duration may have limited the ability to detect group differences, as minimal thrombus deposition was observed in both the CuBTTri and CTRL group over the course of 6 h. This highlights the importance of conducting *in vivo* tests for durations that replicate the typical multi-day duration of extracorporeal lung support, which is currently ongoing in our laboratory.

3.5 Stability and Activity Evaluation of Composite Coating After Blood Exposure

The composite coating was evaluated for stability and activity after exposure to blood flow during the *ex vivo* testing of the tubing. The coating did not exhibit any indication of delamination after visual evaluation by SEM. NO generation from GSNO by the CuBTTri coating was used as a proxy for coating activity. The activity of the coatings was quantified for representative tubing samples pre-blood exposure ($2 \pm 2 \times 10^{-8}$ mol NO, n=8) and post-blood exposure ($8 \pm 7 \times 10^{-9}$ mol NO, n=8) and compared to the control ($2 \pm 2 \times 10^{-10}$ mol NO, n=3) over a 1-h interval. The majority of samples (70%) were measured to have activity above the baseline control (GSNO + circuit tubing alone). While we expected 100% activity, it is possible that due to the heterogeneity of the samples or other molecules adhering to the surface, the bench-top measured activity in some samples was below the limit of detection. Regardless, this may not be a reflection of *ex vivo* activity and requires further evaluation.

4. Conclusion

In conclusion, we successfully established a stable and active CuBTTri composite coating on medical tubing with the potential to decrease thrombus formation. The coating showed no signs of delamination when exposed to flow rates used during partial lung support (up to 2.5 L/min). The stability of the CuBTTri remains in question as we witnessed a small increase in copper during flow experiments. During hemocompatibility testing, no adverse effects were noted, and minimal thrombus deposition occurred. Additionally, the CuBTTri within the coating generated NO in the presence of a biological NO donor, confirming the activity of the MOF after exposure to blood. This composite is promising and could potentially be used to decrease blood clotting on other blood-contacting medical devices as well. Further *in vivo* studies of the efficacy and safety of this approach carried out to a clinically relevant timeline for extracorporeal organ support are required and are currently in progress.

CHAPTER 2

REFERENCES

- [1] J. Andrews and A. M. Winkler, “Challenges with Navigating the Precarious Hemostatic Balance during Extracorporeal Life Support: Implications for Coagulation and Transfusion Management,” *Transfus Med Rev*, vol. 30, no. 4, pp. 223–229, Oct. 2016, doi: 10.1016/j.tmr.2016.07.005.
- [2] T. R. Roberts, M. R. S. Garren, H. Handa, and A. I. Batchinsky, “Toward an artificial endothelium: Development of blood-compatible surfaces for extracorporeal life support,” *J Trauma Acute Care Surg*, vol. 89, no. 2S Suppl 2, pp. S59–S68, Aug. 2020, doi: 10.1097/TA.0000000000002700.
- [3] L.-C. Xu, J. W. Bauer, and C. A. Siedlecki, “Proteins, platelets, and blood coagulation at biomaterial interfaces,” *Colloids and Surfaces B: Biointerfaces*, vol. 124, pp. 49–68, Dec. 2014, doi: 10.1016/j.colsurfb.2014.09.040.
- [4] C. A. Labarrere, A. E. Dabiri, and G. S. Kassab, “Thrombogenic and Inflammatory Reactions to Biomaterials in Medical Devices,” *Front. Bioeng. Biotechnol.*, vol. 8, p. 123, Mar. 2020, doi: 10.3389/fbioe.2020.00123.
- [5] H. J. Dalton *et al.*, “Factors Associated with Bleeding and Thrombosis in Children Receiving Extracorporeal Membrane Oxygenation,” *Am J Respir Crit Care Med*, vol. 196, no. 6, pp. 762–771, Sep. 2017, doi: 10.1164/rccm.201609-1945OC.
- [6] B. Steinlechner *et al.*, “Can Heparin-Coated ECMO Cannulas Induce Thrombocytopenia in COVID-19 Patients?,” *Case Reports in Immunology*, vol. 2021, pp. 1–5, Jun. 2021, doi: 10.1155/2021/6624682.

- [7] P. Gresele, S. Momi, and G. Guglielmini, “Nitric oxide-enhancing or -releasing agents as antithrombotic drugs,” *Biochemical Pharmacology*, vol. 166, pp. 300–312, Aug. 2019, doi: 10.1016/j.bcp.2019.05.030.
- [8] M. W. Radomski and S. Moncada, “The biological and pharmacological role of nitric oxide in platelet function,” *Adv Exp Med Biol*, vol. 344, pp. 251–264, 1993, doi: 10.1007/978-1-4615-2994-1_20.
- [9] V. I. Isaeva and L. M. Kustov, “The application of metal-organic frameworks in catalysis (Review),” *Pet. Chem.*, vol. 50, no. 3, pp. 167–180, May 2010, doi: 10.1134/S0965544110030011.
- [10] J. L. Harding, J. M. Metz, and M. M. Reynolds, “A Tunable, Stable, and Bioactive MOF Catalyst for Generating a Localized Therapeutic from Endogenous Sources,” *Adv. Funct. Mater.*, vol. 24, no. 47, pp. 7503–7509, Dec. 2014, doi: 10.1002/adfm.201402529.
- [11] M. J. Neufeld, B. R. Ware, A. Lutzke, S. R. Khetani, and M. M. Reynolds, “Water-Stable Metal–Organic Framework/Polymer Composites Compatible with Human Hepatocytes,” *ACS Appl. Mater. Interfaces*, vol. 8, no. 30, pp. 19343–19352, Aug. 2016, doi: 10.1021/acsami.6b05948.
- [12] A. Demessence, D. M. D’Alessandro, M. L. Foo, and J. R. Long, “Strong CO₂ Binding in a Water-Stable, Triazolate-Bridged Metal–Organic Framework Functionalized with Ethylenediamine,” *J. Am. Chem. Soc.*, vol. 131, no. 25, pp. 8784–8786, Jul. 2009, doi: 10.1021/ja903411w.
- [13] Y. Zang, T. R. Roberts, A. I. Batchinsky, and M. M. Reynolds, “Metal–Organic Framework Polymer Coating Inhibits *Staphylococcus aureus* Attachment on Medical Circulation

- Tubing under Static and Dynamic Flow Conditions,” *ACS Appl. Bio Mater.*, vol. 3, no. 6, pp. 3535–3543, Jun. 2020, doi: 10.1021/acsabm.0c00151.
- [14] A. J. Boyle *et al.*, “Extracorporeal carbon dioxide removal for lowering the risk of mechanical ventilation: research questions and clinical potential for the future,” *Lancet Respir Med*, vol. 6, no. 11, pp. 874–884, Nov. 2018, doi: 10.1016/S2213-2600(18)30326-6.
- [15] N. J. Prat *et al.*, “Low-Dose Heparin Anticoagulation During Extracorporeal Life Support for Acute Respiratory Distress Syndrome in Conscious Sheep,” *Shock*, vol. 44, no. 6, pp. 560–568, Dec. 2015, doi: 10.1097/SHK.0000000000000459.
- [16] T. R. Roberts *et al.*, “Tethered Liquid Perfluorocarbon Coating for 72 Hour Heparin-Free Extracorporeal Life Support,” *ASAIO Journal*, vol. Publish Ahead of Print, Feb. 2021, doi: 10.1097/MAT.0000000000001292.
- [17] T. R. Roberts *et al.*, “Heparin-Free Extracorporeal Life Support Using Tethered Liquid Perfluorocarbon: A Feasibility and Efficacy Study,” *ASAIO Journal*, vol. 66, no. 7, pp. 809–817, Jul. 2020, doi: 10.1097/MAT.0000000000001055.
- [18] G. Wyszogrodzka, B. Marszałek, B. Gil, and P. Dorożyński, “Metal-organic frameworks: mechanisms of antibacterial action and potential applications,” *Drug Discovery Today*, vol. 21, no. 6, pp. 1009–1018, Jun. 2016, doi: 10.1016/j.drudis.2016.04.009.
- [19] D. Abrams, R. Roncon-Albuquerque, and D. Brodie, “What’s new in extracorporeal carbon dioxide removal for COPD?,” *Intensive Care Med*, vol. 41, no. 5, pp. 906–908, May 2015, doi: 10.1007/s00134-015-3677-5.
- [20] T. C. Major *et al.*, “The hemocompatibility of a nitric oxide generating polymer that catalyzes S-nitrosothiol decomposition in an extracorporeal circulation model,”

- Biomaterials*, vol. 32, no. 26, pp. 5957–5969, Sep. 2011, doi:
10.1016/j.biomaterials.2011.03.036.
- [21] M. J. Neufeld, A. Lutzke, W. M. Jones, and M. M. Reynolds, “Nitric Oxide Generation from Endogenous Substrates Using Metal–Organic Frameworks: Inclusion within Poly(vinyl alcohol) Membranes To Investigate Reactivity and Therapeutic Potential,” *ACS Appl. Mater. Interfaces*, vol. 9, no. 41, pp. 35628–35641, Oct. 2017, doi:
10.1021/acsami.7b11846.
- [22] D. Tsikas, “Measurement of physiological S-nitrosothiols: a problem child and a challenge,” *Nitric Oxide*, vol. 9, no. 1, pp. 53–55, Aug. 2003, doi: 10.1016/s1089-8603(03)00044-2.
- [23] E. Nagababu and J. M. Rifkind, “Routes for Formation of S-Nitrosothiols in Blood,” *Cell Biochem Biophys*, vol. 67, no. 2, pp. 385–398, Nov. 2013, doi: 10.1007/s12013-011-9321-2.
- [24] M. E. Douglass *et al.*, “Catalyzed Nitric Oxide Release via Cu Nanoparticles Leads to an Increase in Antimicrobial Effects and Hemocompatibility for Short-Term Extracorporeal Circulation,” *ACS Appl. Bio Mater.*, vol. 2, no. 6, pp. 2539–2548, Jun. 2019, doi:
10.1021/acsabm.9b00237.
- [25] X. M. Mueller, H. T. Tevæarai, D. Jegger, O. Tucker, and L. K. von Segesser, “Are standard human coagulation tests suitable in pigs and calves during extracorporeal circulation?,” *Artif Organs*, vol. 25, no. 7, pp. 579–584, Jul. 2001, doi: 10.1046/j.1525-1594.2001.025007579.x.

- [26] M. M. Bembea, G. Annich, P. Rycus, G. Oldenburg, I. Berkowitz, and P. Pronovost, “Variability in anticoagulation management of patients on extracorporeal membrane oxygenation: an international survey,” *Pediatr Crit Care Med*, vol. 14, no. 2, pp. e77-84, Feb. 2013, doi: 10.1097/PCC.0b013e31827127e4.

CHAPTER 3

SURFACE MODIFICATION OF OXYGENATOR FIBERS WITH A CATALYTICALLY ACTIVE METAL-ORGANIC FRAMEWORK TO GENERATE NO FROM GSNO

1. Introduction

Extracorporeal circuits utilize blood-contacting medical devices and components to provide organ support to the heart, lungs, kidneys, and/or liver. Specifically, extracorporeal membrane oxygenation (ECMO) supports patients suffering from severe cardiovascular or pulmonary failures. Blood is drawn from a patient and is circulated through an oxygenator using medical tubing. The oxygenator performs gas exchange, returning oxygen rich blood to the vasculature of the patient [1]. Despite decades of research and technological advancements, ECMO still has significant limitations, mainly due to hemorrhagic and thrombotic complications [2]. When blood comes into contact with the hydrophobic components of the circuit, proteins adsorb to the surface leading to the adsorption, activation, and aggregation of platelets, eventually forming a thrombus [3]. In particular, the oxygenator contributes approximately 90% of the surface area contacted by blood, ranging between 0.8-2.5 m², which has led to oxygenator thrombosis in 10-16% of patients [2], [4], [5]. Currently, the standard method to decrease thrombotic complications is to administer a systemic anticoagulant such as unfractionated heparin; however, this causes a new series of hemorrhagic issues such as heparin-induced thrombocytopenia [6].

Nitric oxide (NO) is a molecule produced by endothelial cells which has been shown to inhibit platelet activation and aggregation within the vasculature [7]. For this reason, there have been many reported examples of NO releasing materials to be coated onto different ECMO

components [8], [9]. For example, Winnersbach et al. coated the fibers within the oxygenator with a NO-releasing hydrogel, and found the amount of platelets adhering to the fibers decreased after 48 minutes of blood exposure [8]. While the results of these studies are promising by showing a decrease in thrombotic activity, the NO reservoirs within the coatings only last for a short period of time. This could be problematic as ECMO is a long-term life support system and might be needed for weeks. The current study uses a different approach to mimic the endothelium by taking advantage of a catalytic mechanism to generate NO from an endogenous source.

S-nitrosothiols (RSNOs) are a group of stable endogenous molecules which serve as a natural reservoir for NO [10]. These RSNOs are present in a μM concentration within blood and can release NO from a number of different reactions, including a catalytic reaction from copper [11], [12]. This study aims to create a coating for the fibers within the oxygenator using a copper-based metal organic framework, $\text{H}_3[(\text{Cu}_4\text{Cl})_3(\text{BTri})_8(\text{H}_2\text{O})_{12}] \cdot 72\text{H}_2\text{O}$ where $\text{H}_3\text{BTri} = 1,3,5\text{-tris}(1H\text{-}1,2,3\text{-triazole-}5\text{-yl)benzene}$ (CuBTri), as a source of copper to catalytically generate NO from *s*-nitrosoglutathione (GSNO), an endogenous RSNO. CuBTri was chosen because previous reports have shown it to be stable under biological conditions and compatible with human cells, unlike other copper-based MOFs or materials [13].

Within this study, we used a mussel-inspired molecule, polydopamine (PDA), to create an adherent layer on polymethylpentene (PMP) oxygenator fibers to immobilize CuBTri. The inspiration for using PDA as a functionalized polymeric coating comes from the catechol molecule, dopa, which mussels use to cling to many different surfaces even when surrounded by water [14], [15]. The polymer has been used to coat oxygenator fibers before, as it will enhance the hydrophilicity of the surface and therefore increase the biocompatibility. Specifically, Leung

et al. coated polydimethylsiloxane oxygenator fibers with PDA and an antithrombin-heparin complex, which displayed hydrophilic water contact angles and inhibited Factor Xa within the blood clotting mechanism [16]. Additionally, Jiang et al. used a PDA layer on a porous polyethylene porous membrane to immobilize heparin; this group displayed increased hydrophilicity of the surface and decreased adhesion and activation of platelets due to the immobilized heparin [17]. Finally, Fan et al. reported the use of PDA to immobilize a different copper-based MOF, copper(II) benzene-1,3,5-tricarboxylate (CuBTC), on cardiovascular stents, and found sufficient NO release; however, while this study took advantage of the degradation properties of CuBTC to release copper ions, we attempt to use the aqueous stability of CuBTTri so limited amounts of copper ions are released [18].

Within this report, PDA is used as an adhesive layer to immobilize catalytically active CuBTTri on PMP oxygenator fibers. We have evaluated the morphology of the coating and have shown that the CuBTTri within the coating is able to generate NO in the presence of GSNO at a flux similar to the natural endothelium. To our knowledge, this is the first time a copper-based MOF has been immobilized using PDA for anticoagulation purposes within an extracorporeal circuit.

2. Materials and Methods

2.1 Materials

All materials were purchased from vendors as specified. 1,3,5-triethynylbenzene (98%) and copper(II) chloride dihydrate (99%, $\text{CuCl}_2 \cdot \text{H}_2\text{O}$) were purchased from Alfa Aesar (Ward Hill, MA). Copper(I) iodide (>99.5%, CuI) was purchased from Sigma-Aldrich (St. Louis, MO). Methanol (99.9%), sodium chloride (99.0%), sodium hydroxide (98.9%), and tris hydrochloride were purchased from Fisher Scientific (Hampton, NH). Diethyl ether (>99.0%) was purchased

from Millipore Sigma (Burlington, MA). N,N-dimethylformamide (99.8%, DMF) was purchased from VWR International (Radnor, PA). Trimethylsilyl azide (>95.0%) and 3-Hydroxytyramine Hydrochloride (>98.0%, dopamine HCl) were purchased from Tokyo Chemical Industry (Tokyo, Japan). Ultrapure water (18.2 M Ω ·cm) was supplied from Millipore MilliQ-IQ water purification system (Billerica, MA). The polymethylpentene fibers were taken from the Maquet HLS Set Advanced 7.0 oxygenator (Rastatt, Germany).

2.2 *CuBTri Composite Preparation*

2.2.1 *CuBTri Synthesis*

The synthesis of H₃[(Cu₄Cl)₃(BTri)₈·(H₂O)₁₂]·72H₂O (CuBTri) was based on a reported method [19]. Briefly, 1,3,5-triethynylbenzene (5.3 g, 35.29 mmol) and CuI (1.011 g, 5.31 mmol) were added to a solution of DMF (180 mL) and methanol (20 mL) and mixed under a nitrogen atmosphere. Trimethylsilyl azide (21 mL, 158.95 mmol) was added, and the reaction was heated to 100°C for 36-48 h. Rotary evaporation was used to remove any excess solvent. The precipitate, 1,3,5-tris(1H-1,2,3-triazol-5-yl)-benzene (H₃BTri), was collected via filtration then washed with 500 mL each of H₂O and diethyl ether.

A solution of H₃BTri (1.2375 g, 5.1535 mmol) and DMF (220 mL) was sonicated for 1 h. CuCl₂·H₂O (2.1065 g, 12.36 mmol) was added to the mixture then heated to 100°C for 72 h. The final CuBTri product, a purple precipitate, was collected using a fine porosity fritted glass funnel and washed with 100 mL each of DMF and water. The filtered solid was heated in 200 mL of water for 24 h at 95°C. The solid was filtered, washed with 100 mL of water, and heated for 24 h at 95 °C three separate times. After the final water wash, the product was dried under a partial vacuum then hand-ground for 10 min.

2.2.2 Coating Procedure

A schematic of the coating procedure is shown in Figure 3.1. A sample from the PMP fibers was taken from the oxygenator (Maquet, Rastatt, Germany) and were cut into square pieces (1.5 cm by 1.5 cm) before being rinsed with Ultrapure water. The fiber sample was put under vacuum for 24 h to evaporate any excess water. Afterward, 20 mg of dopamine HCl was added to 10 mL of 10 mM tris-HCl solution (pH = 8.5). The fiber sample was added to the solution and agitated for 24 h. During this time, polymerization of dopamine occurred to form an adhesive polydopamine (PDA) layer. Afterwards, the fiber sample was agitated in Ultrapure water for 24 h to rinse off any unbound PDA. This process was repeated two more times to achieve a three-layer PDA coating. Then, 20 mg of CuBTTri was added to 10 mL of water. The fiber sample was added to this CuBTTri solution and agitated for 24 h. In a final washing step, the sample was agitated in Ultrapure water for 24 h before being put under vacuum for 24 h.

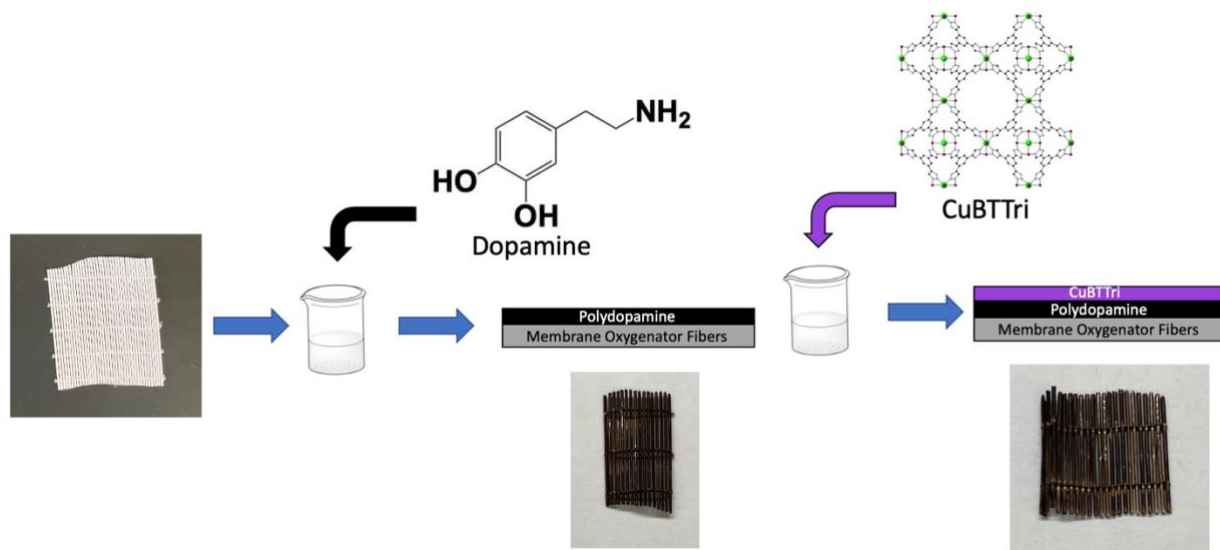


Figure 3.1. Schematic of the coating procedure. Fibers were placed in a solution of dopamine before being placed in a solution of CuBTTri to immobilize the CuBTTri on the fibers.

2.3 Coating Characterization

Fourier-transform infrared spectroscopy (FTIR, Thermo-Nicolette 6700) was used to measure the changes in functional groups on the fiber surface before and after PDA was coated. Samples were analyzed in a from 650 cm^{-1} to 4000 cm^{-1} .

Coating morphology of the fibers was assessed via scanning electron microscopy (SEM) imaging. A JEOL JSM-6500F scanning electron microscope (Akishima, Tokyo, Japan) was used with an accelerating voltage of 5.0 kV at magnifications of 1000x. The samples were sputter-coated with 20 nm of gold before imaging (n=6). Energy-dispersive x-ray spectroscopy (EDS) images were obtained using the same instrument with an Oxford X-max 80 mm² attachment. An accelerating voltage of 15.0 kV was used, at 1000x magnification. EDS was used to scan the images for copper content on the surface (n=3).

2.4 Coating Activity Analysis

The fibers were assessed for CuBTTri catalytic activity by analyzing NO release from GSNO. Nitric Oxide Analyzers (280i, Zysense, Weddington, North Carolina) were used to track GSNO oxidation via chemiluminescence-based NO detection. Samples were submerged in 5 mL of Ultrapure water maintained at 38°C within a covered reaction cell. 10 μM GSNO was injected into the reaction cell, and the reaction proceeded for at least 200 mins with constant nitrogen bubbling and a collection interval of 1 s. Within the timeframe of each experiment (ranging between 200-500 mins), there was at least 125 mins where the NO flux remained relatively constant (only differentiating by a maximum of $0.02\text{ nmol/min/cm}^2$). Therefore, NO fluxes were calculated by using the average flux in the experiment that had been maintained for at least a 125 mins (n=6). These values were compared to controls using uncoated fibers (n=3) and PDA coated fibers (n=3).

2.5 Multi-day Stability Testing

2.5.1 Assessment of MOF Stability in Saline

Saline stability tests were performed to determine if the CuBTTri on the coating remained stable in dynamic conditions. The coated mesh fibers were placed in 10 mL of 0.9% saline solution (0.09 g in 10 mL of Ultrapure water) and agitated for 72 h. Inductively coupled plasma mass spectroscopy (ICP-MS, NexION 350D, PerkinElmer, Waltham, MA) was used to evaluate the stability of CuBTTri by measuring copper concentration after the test was performed (n=6) to determine if the MOF was degrading into copper ions and H₃BTTri. The copper concentration was compared to the same experiments using uncoated fibers (n=3) and PDA coated fibers (n=3).

2.5.2 Assessment of MOF Activity After Stability Testing

Additionally, the CuBTTri coated fibers were analyzed for their activity after stability tests using the same methods as discussed in section 2.4 (n=6). The NO fluxes were compared to the fluxes assessed before the stability experiment was performed.

2.6 Statistical Analysis

For coating activity tests and MOF stability tests, statistical differences were analyzed with a two-tailed t-test ($\alpha \leq 0.05$). Each data point with the CuBTTri coated fibers was repeated 6 times, and the controls were repeated 3 times. The average and standard deviation are reported.

3. Results and Discussion

We aimed to engineer a bioactive coating for the fibers present within the oxygenator of ECMO. The bioactive coating consists of polydopamine (PDA), which acts as a “bioglue” [16] to immobilize the CuBTri on the fibers. A PDA coating was prepared by agitating a sample of the oxygenator fibers in dopamine HCl three times, each followed by a wash in Ultrapure water. The CuBTri was immobilized onto the PDA coating by agitating the fibers in a solution of CuBTri. The MOF within this coating was determined to catalytically generate NO from GSNO both before and after stability testing.

3.1 Coating Evaluation

The coating was analyzed first visually and then using FTIR to determine if the PDA was present on the surface. Figure 3.2 shows the original white fibers (left) compared to the layered coating formed by black PDA on the surface of the fibers (right) [20]. FTIR spectra were taken of the uncoated polymethylpentene (PMP) fibers, and the PDA coated fibers as seen in Figure 3.3. Features of the FTIR indicate the presence of PDA and allow us to conclude PDA was successfully coated on the fibers. Features observed in both the uncoated and coated fibers included 2925 cm^{-1} , 1460 cm^{-1} , and 1354 cm^{-1} corresponding to $\nu(\text{C-H})$, $\nu_{ring}(\text{C=C})$, and $\nu_{ring}(\text{CNC})$ respectively. These wavenumbers are consistent with previous work done with PMP [21]. The features observed in the PDA coated fibers includes a broad band at $3650\text{-}3250\text{ cm}^{-1}$ which corresponds to the stretching between (N-H) and (O-H), and 1596 cm^{-1} and 1510 cm^{-1} which corresponds to the $(\text{C=C})_{ring}$, and $(\text{C=N})_{ring}$ respectively. These wavenumbers are consistent with previous work done with PDA [22].

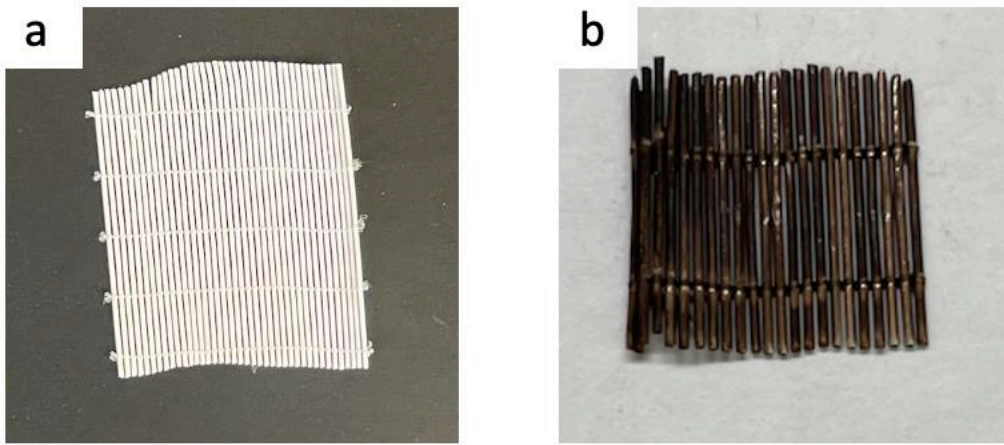


Figure 3.2. 1.5 x 1.5 cm samples of the white uncoated fibers (a) and the PDA coated fibers (b). The color change is indicative of successfully coating PDA onto the fibers.

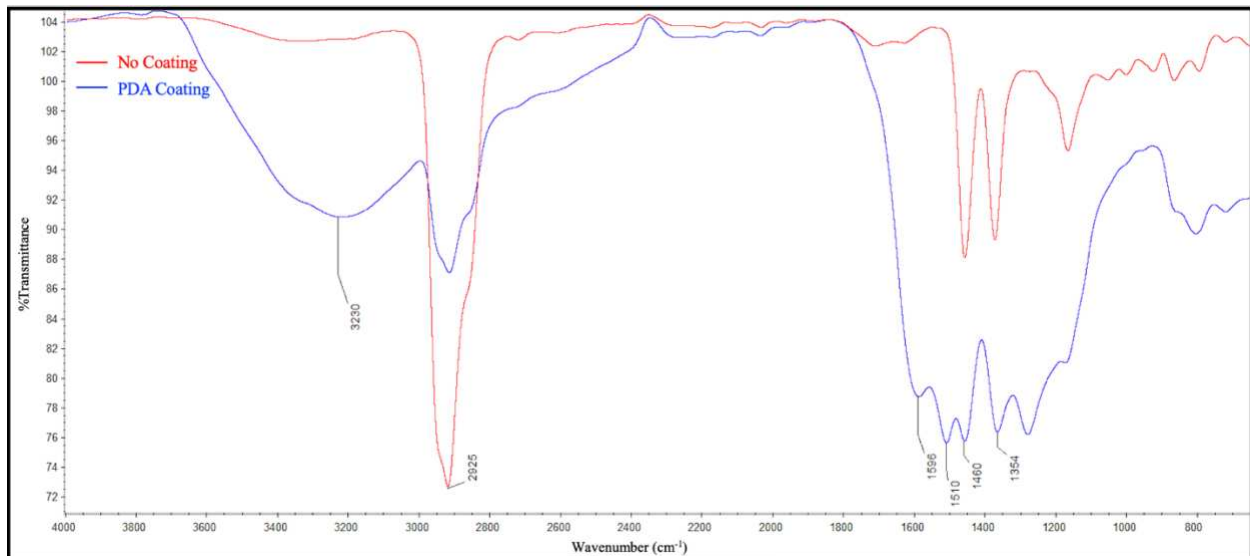


Figure 3.3. FTIR spectra of the PMP uncoated fibers (red) and the PDA coated fibers (blue). The broad peak from 3650-3250 cm^{-1} and the peaks at 1596 cm^{-1} and 1510 cm^{-1} indicate the fibers were successfully coated with PDA.

SEM coupled with EDS was used to assess if the CuBTri was present on the fibers after the coating procedure. Figure 3.4 shows SEM images of the non-coated, PDA-coated, and PDA/CuBTri coated fibers at 1,000x magnification. The EDS mapping in Figure 3.5a-3.5f shows the presence of carbon, copper, nitrogen, and oxygen on the surface of the PDA/CuBTri coated fibers; these images were taken at 1,000x magnification. The large particles seen in the SEM image correlate with the higher density points of the copper-mapped EDS image, indicating that these particles are in fact CuBTri, as there was no other source of copper applied to the coating. Additionally, the nitrogen and oxygen mapped EDS images further allowed us to confirm the presence of the PDA on the surface of the fibers. There is one high density point on the oxygen-mapped EDS image, which could be due to excess oxygen adhering the MOF particles or other debris on the surface. It can be seen in all the SEM images that the CuBTri particles are dispersed across the surface area of the fibers, which is optimal to generate dispersed amounts of NO to decrease blood clotting.

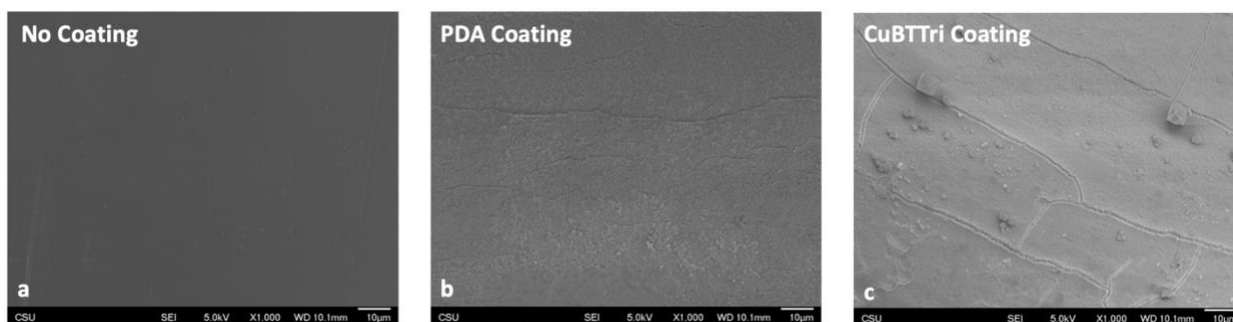


Figure 3.4. Representative SEM images of the oxygenator fibers. Images were taken of (a) non-coated fibers (b) PDA coated fibers, and (c) PDA/CuBTri coated fibers.

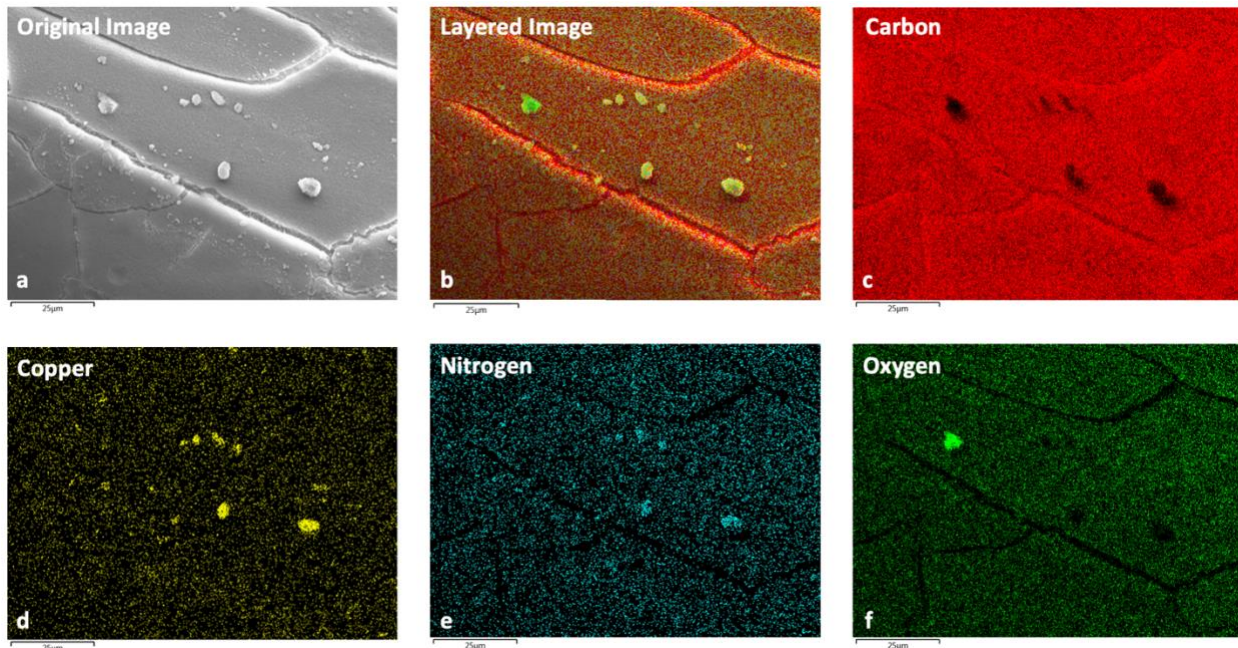


Figure 3.5. Representative SEM-EDS images to show the elemental content of the PDA/CuBTri coated fibers using 1,000x magnification. (a) Original SEM Image of the PDA/CuBTri coated fibers. (b) EDS map image of carbon, copper, nitrogen, and oxygen on top of each other. EDS maps of carbon (c), copper (d), nitrogen (e), and oxygen (f).

3.2 Coating Activity Analysis

The primary success of the coating is reliant on if the CuBTri within the coating catalyzes the release of NO from an endogenously present NO donor. This analysis was done by submerging the coated fibers into a 10 μM solution of GSNO. The average fluxes for the non-coated fibers and PDA coated fibers were $0.00035 \pm 0.00032 \text{ nmol/min/cm}^2$ ($n=3$) and $0.00062 \pm 0.00081 \text{ nmol/min/cm}^2$ ($n=3$) respectively. The flux increased to $0.10 \pm 0.03 \text{ nmol/min/cm}^2$ ($n=6$) for the CuBTri coated fibers. This is within the range of endothelial NO flux ($0.05\text{-}0.4 \text{ nmol/min/cm}^2$) [23]. Importantly, a consistent NO flux occurred for an average of 187.5 mins (and at least 125 mins) across all experiments, inferring that the coating can consistently generate NO in the presence of GSNO. The experiments are not expected to last for longer periods of time as a single GSNO molecule can only generate one NO molecule; therefore, eventually the NO

donor is exhausted. Other blood-contacting applications have also used copper coatings to release NO from GSNO. These applications report average or maximum NO fluxes between 0.07-1.20 nmol/min/cm², but use different concentrations of copper as well as GSNO/glutathione mixtures which could explain major deviations between results [18], [24]–[26]. There are very limited examples of NO releasing coatings for the fibers on the oxygenator. One example is reported by El-Ferzli et al.; this group developed a NO releasing, self-assembled peptide amphiphile matrix on polypropylene fibers which showed a decrease in platelet adhesion compared to the uncoated controls [27]. The NO flux generated by the CuBTTri has the potential to decrease platelet adhesion and aggregation on the oxygenator.

3.3 MOF Stability

It was previously reported that some copper-based MOFs are not stable under aqueous conditions and degrade into copper ions and their associated ligand when exposed to water [28]. CuBTTri has been shown to be stable in aqueous conditions [13], but has not been thoroughly tested in a dynamic aqueous environment. Samples of the fibers (non-coated, PDA coated, and PDA/CuBTTri coated) were separately agitated in 0.9% saline solutions for 72 h to determine if the CuBTTri degraded into copper ions and a ligand. The copper concentrations for the fiber samples with no coating, PDA coating, and PDA/CuBTTri coating were 6.5 ± 1.5 ng/mL (n=3), 3.9 ± 1.2 ng/mL (n=3), and 14.5 ± 10.3 ng/mL (n=6) respectively, as seen in Figure 3.6. There was no statistical difference in copper concentration for the fibers with PDA coating or PDA/CuBTTri coating as compared to the control with no coating ($p > 0.05$). However, two of the experiments containing CuBTTri coated fibers displayed a large increase in copper concentration (hence the larger mean and standard deviation) which could be indicative of MOF degradation or exposure of unbound copper ions left over from the MOF synthesis. Additional

experimentation will need to be conducted to determine which is occurring. There have been other methods which use copper as a catalyst for NO release and found large amounts of leached copper. For example, Major et al. developed a copper-nanoparticle-containing polymer for extracorporeal circulation and found 234 ± 80 ng/mL of copper after 7 days in their saline stability experiment [24]. Within this study, it is mentioned that the U.S. Institute of Medicine recommends a daily copper intake of 900 μ g/day with a high tolerance level of 10,000 μ g/day in adults, so the small amount of excess copper may not be a safety issue [24], [29]. Similarly, the possible MOF degradation might not result in clinical concerns, but further tests would be beneficial to ensure the safety of the device.

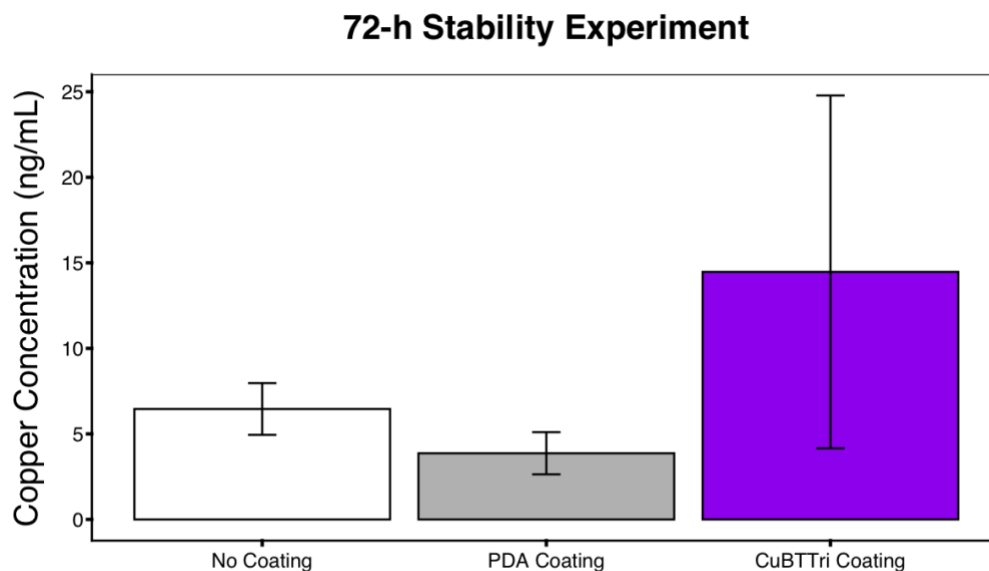


Figure 3.6. Stability testing to determine if the CuBTri within the coating degrades under agitation. Copper concentrations are shown for fibers with no coating, PDA coating, and PDA/CuBTri coating.

Additionally, the activity of the CuBTri was assessed after stability experiments to ensure that the MOF remained immobilized on the fibers and the NO generation was not

affected. The average flux of NO generation for the PDA/CuBTtri coated fibers before and after the 72-h stability experiment was 0.10 ± 0.03 nmol/min/cm² (n=6) and 0.09 ± 0.01 nmol/min/cm² (n=6), with no statistical difference between the two experiments ($p > 0.05$). A representative image of the NO release over time is displayed in Figure 3.7, comparing the CuBTtri coating before (blue) and after (red) the 72-h stability test. We were able to conclude that the CuBTtri remained immobilized on the fibers and the catalytic function was not affected.

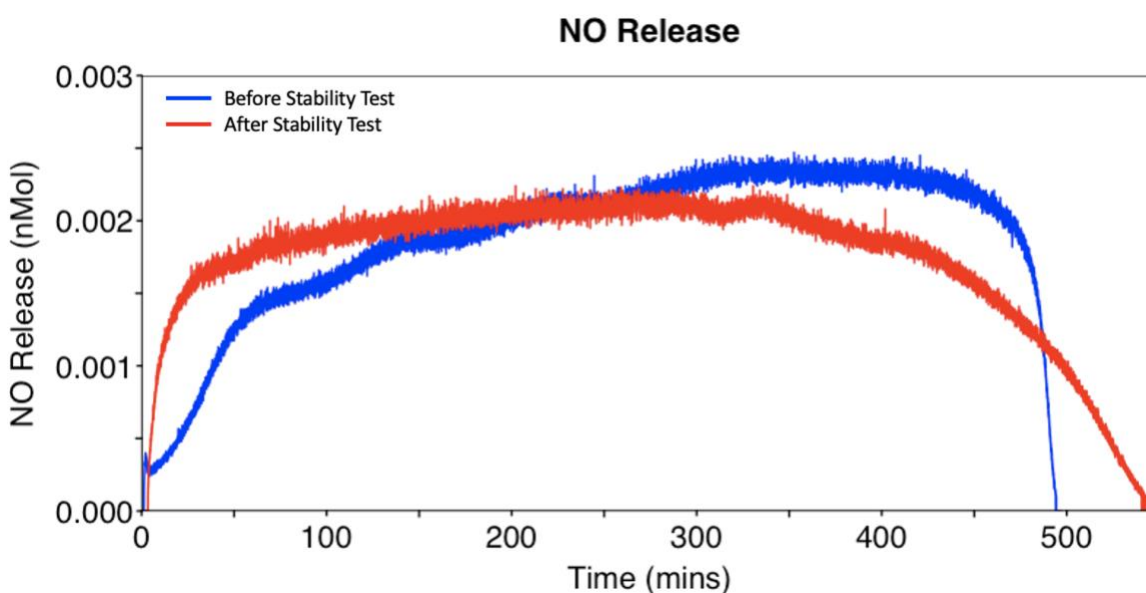


Figure 3.7. Representative NO release of the PDA/CuBTtri coating before (blue) and after (red) the 72-h saline stability test.

4. Conclusion

In summary, we have developed a process to immobilize catalytically active CuBTtri on the surface of PMP oxygenator fibers using an adherent PDA layer. The PMP surface was modified with PDA which contains adhesive properties to immobilize CuBTtri particles. The CuBTtri was shown to be dispersed across the surface area of the fibers, which is important to generate dispersed quantities of NO throughout the entire oxygenator. The incorporation of the

CuBTTri increased the NO generation from 0.00035 ± 0.00032 nmol/min/cm² to 0.10 ± 0.03 nmol/min/cm², demonstrating that the MOF is catalytically active. This NO flux is similar to that of the endothelium and is maintained for at least 125 mins in the presence of GSNO. The stability of the CuBTTri in dynamic aqueous conditions is still unclear, but the MOF will remain on the surface of the fibers and still be catalytically active after aqueous dynamic agitation. Overall, we found that the inclusion of CuBTTri on the surface of PMP oxygenator fibers increases the NO generation and believed this localized NO flux can be used to decrease the thrombotic tendencies within the oxygenator to provide a safer life support system.

CHAPTER 3

REFERECNES

- [1] L. Lequier, S. B. Horton, D. M. McMullan, and R. H. Bartlett, “Extracorporeal Membrane Oxygenation Circuitry,” *Pediatr Crit Care Med*, vol. 14, no. 5 0 1, pp. S7-12, Jun. 2013, doi: 10.1097/PCC.0b013e318292dd10.
- [2] A. J. Doyle and B. J. Hunt, “Current Understanding of How Extracorporeal Membrane Oxygenators Activate Haemostasis and Other Blood Components,” *Frontiers in Medicine*, vol. 5, 2018, Accessed: Apr. 29, 2022. [Online]. Available: <https://www.frontiersin.org/article/10.3389/fmed.2018.00352>
- [3] L.-C. Xu, J. W. Bauer, and C. A. Siedlecki, “Proteins, platelets, and blood coagulation at biomaterial interfaces,” *Colloids and Surfaces B: Biointerfaces*, vol. 124, pp. 49–68, Dec. 2014, doi: 10.1016/j.colsurfb.2014.09.040.
- [4] T. M. Maul, M. P. Massicotte, and P. D. Wearden, *ECMO Biocompatibility: Surface Coatings, Anticoagulation, and Coagulation Monitoring*. IntechOpen, 2016. doi: 10.5772/63888.
- [5] M. Zhang *et al.*, “Anti-thrombogenic Surface Coatings for Extracorporeal Membrane Oxygenation: A Narrative Review,” *ACS Biomater. Sci. Eng.*, vol. 7, no. 9, pp. 4402–4419, Sep. 2021, doi: 10.1021/acsbomaterials.1c00758.
- [6] K. Giuliano *et al.*, “Extracorporeal Membrane Oxygenation Complications in Heparin- and Bivalirudin-Treated Patients,” *Crit Care Explor*, vol. 3, no. 7, p. e0485, Jul. 2021, doi: 10.1097/CCE.0000000000000485.

- [7] J. Loscalzo, “Nitric Oxide Insufficiency, Platelet Activation, and Arterial Thrombosis,” *Circulation Research*, vol. 88, no. 8, pp. 756–762, Apr. 2001, doi: 10.1161/hh0801.089861.
- [8] P. Winnersbach *et al.*, “Endogenous Nitric Oxide-Releasing Microgel Coating Prevents Clot Formation on Oxygenator Fibers Exposed to In Vitro Blood Flow,” *Membranes (Basel)*, vol. 12, no. 1, p. 73, Jan. 2022, doi: 10.3390/membranes12010073.
- [9] T. C. Major *et al.*, “The effect of a polyurethane coating incorporating both a thrombin inhibitor and nitric oxide on hemocompatibility in extracorporeal circulation,” *Biomaterials*, vol. 35, no. 26, pp. 7271–7285, Aug. 2014, doi: 10.1016/j.biomaterials.2014.05.036.
- [10] J. S. Stamler *et al.*, “Nitric oxide circulates in mammalian plasma primarily as an S-nitroso adduct of serum albumin.,” *Proc Natl Acad Sci U S A*, vol. 89, no. 16, pp. 7674–7677, Aug. 1992.
- [11] J. S. Stamler, “S-Nitrosothiols in the Blood,” *Circulation Research*, vol. 94, no. 4, pp. 414–417, Mar. 2004, doi: 10.1161/01.RES.0000122071.55721.BC.
- [12] D. L. H. Williams, “The Chemistry of S-Nitrosothiols,” *Acc. Chem. Res.*, vol. 32, no. 10, pp. 869–876, Oct. 1999, doi: 10.1021/ar9800439.
- [13] M. J. Neufeld, B. R. Ware, A. Lutzke, S. R. Khetani, and M. M. Reynolds, “Water-Stable Metal–Organic Framework/Polymer Composites Compatible with Human Hepatocytes,” *ACS Appl. Mater. Interfaces*, vol. 8, no. 30, pp. 19343–19352, Aug. 2016, doi: 10.1021/acsami.6b05948.
- [14] B. P. Lee, P. B. Messersmith, J. N. Israelachvili, and J. H. Waite, “Mussel-Inspired Adhesives and Coatings,” *Annu Rev Mater Res*, vol. 41, pp. 99–132, Aug. 2011, doi: 10.1146/annurev-matsci-062910-100429.

- [15] Y. H. Ding, M. Floren, and W. Tan, “Mussel-inspired polydopamine for bio-surface functionalization,” *Biosurface and Biotribology*, vol. 2, no. 4, pp. 121–136, Dec. 2016, doi: 10.1016/j.bsbt.2016.11.001.
- [16] J. M. Leung *et al.*, “Surface modification of poly(dimethylsiloxane) with a covalent antithrombin–heparin complex for the prevention of thrombosis: use of polydopamine as bonding agent,” *J. Mater. Chem. B*, vol. 3, no. 29, pp. 6032–6036, Jul. 2015, doi: 10.1039/C5TB00808E.
- [17] J.-H. Jiang, L.-P. Zhu, X.-L. Li, Y.-Y. Xu, and B.-K. Zhu, “Surface modification of PE porous membranes based on the strong adhesion of polydopamine and covalent immobilization of heparin,” *Journal of Membrane Science*, vol. 364, no. 1, pp. 194–202, Nov. 2010, doi: 10.1016/j.memsci.2010.08.017.
- [18] Y. Fan *et al.*, “Immobilization of nano Cu-MOFs with polydopamine coating for adaptable gas transmitter generation and copper ion delivery on cardiovascular stents,” *Biomaterials*, vol. 204, pp. 36–45, Jun. 2019, doi: 10.1016/j.biomaterials.2019.03.007.
- [19] A. Demessence, D. M. D’Alessandro, M. L. Foo, and J. R. Long, “Strong CO₂ Binding in a Water-Stable, Triazolate-Bridged Metal–Organic Framework Functionalized with Ethylenediamine,” *J. Am. Chem. Soc.*, vol. 131, no. 25, pp. 8784–8786, Jul. 2009, doi: 10.1021/ja903411w.
- [20] D. Aguilar-Ferrer, J. Szewczyk, and E. Coy, “Recent developments in polydopamine-based photocatalytic nanocomposites for energy production: Physico-chemical properties and perspectives,” *Catalysis Today*, Aug. 2021, doi: 10.1016/j.cattod.2021.08.016.

- [21] I. Michaljaničová *et al.*, “High power plasma as an efficient tool for polymethylpentene cytocompatibility enhancement,” *RSC Advances*, vol. 6, no. 79, pp. 76000–76010, 2016, doi: 10.1039/C6RA14949A.
- [22] R. A. Zangmeister, T. A. Morris, and M. J. Tarlov, “Characterization of Polydopamine Thin Films Deposited at Short Times by Autoxidation of Dopamine,” *Langmuir*, vol. 29, no. 27, pp. 8619–8628, Jul. 2013, doi: 10.1021/la400587j.
- [23] M. W. Vaughn, L. Kuo, and J. C. Liao, “Estimation of nitric oxide production and reaction rates in tissue by use of a mathematical model,” *Am J Physiol*, vol. 274, no. 6, pp. H2163–2176, Jun. 1998, doi: 10.1152/ajpheart.1998.274.6.H2163.
- [24] T. C. Major *et al.*, “The hemocompatibility of a nitric oxide generating polymer that catalyzes S-nitrosothiol decomposition in an extracorporeal circulation model,” *Biomaterials*, vol. 32, no. 26, pp. 5957–5969, Sep. 2011, doi: 10.1016/j.biomaterials.2011.03.036.
- [25] S. Hwang and M. E. Meyerhoff, “Polyurethane with tethered copper(II)–cyclen complex: Preparation, characterization and catalytic generation of nitric oxide from S-nitrosothiols,” *Biomaterials*, vol. 29, no. 16, pp. 2443–2452, Jun. 2008, doi: 10.1016/j.biomaterials.2008.02.004.
- [26] M. E. Douglass *et al.*, “Catalyzed Nitric Oxide Release via Cu Nanoparticles Leads to an Increase in Antimicrobial Effects and Hemocompatibility for Short-Term Extracorporeal Circulation,” *ACS Appl. Bio Mater.*, vol. 2, no. 6, pp. 2539–2548, Jun. 2019, doi: 10.1021/acsabm.9b00237.

- [27] G. T. El-Ferzli *et al.*, “A Nitric Oxide–Releasing Self-Assembled Peptide Amphiphile Nanomatrix for Improving the Biocompatibility of Microporous Hollow Fibers,” *ASAIO Journal*, vol. 61, no. 5, pp. 589–595, Oct. 2015, doi: 10.1097/MAT.0000000000000257.
- [28] G. Wyszogrodzka, B. Marszałek, B. Gil, and P. Dorożyński, “Metal-organic frameworks: mechanisms of antibacterial action and potential applications,” *Drug Discovery Today*, vol. 21, no. 6, pp. 1009–1018, Jun. 2016, doi: 10.1016/j.drudis.2016.04.009.
- [29] B. R. Stern, “Essentiality and Toxicity in Copper Health Risk Assessment: Overview, Update and Regulatory Considerations,” *Journal of Toxicology and Environmental Health, Part A*, vol. 73, no. 2–3, pp. 114–127, Jan. 2010, doi: 10.1080/15287390903337100.

CHAPTER 4

SUMMARY AND FUTURE DIRECTIONS

1. General Conclusions

The study herein incorporates a copper-based MOF, CuBTTri, onto the surfaces of ECMO components, specifically the tubing and oxygenator fibers, to generate nitric oxide (NO) as a potential therapy for localized coagulation. In the ECMO circuit, the components with the largest blood contacting areas are the tubing and the oxygenator. When blood comes into contact with these components, clots form and can be detrimental to the device or cause further harm to the patient. Two distinct coatings were created to generate localized NO, one for the tubing and one for the fibers within the oxygenator. Historical challenges with coating these components include adhesion of the coating to the underlying tubing or fibers, the durability of the coating, and maintaining the performance of the device by not modifying the physical surface properties. In this thesis, coating processes were developed to adhere CuBTTri to the surfaces of ECMO components. Some of the major challenges include using polymers to properly attach the CuBTTri to the surface while limiting agglomeration and finding a proper coating method which maintains the adhesion of the particles during dynamic experiments. To my knowledge, this is the first time that CuBTTri has been successfully coated onto standard ECMO circuitry tubing and that any MOF has been successfully immobilized on the fibers within the ECMO oxygenator.

2. Conclusions and Future Work for the Tubing

The goal for this study was to engineer a uniform, stable, and active coating for ECMO circulatory tubing. In short, the coating was created by flowing a solution containing dissolved

Tygon polymer and CuBTTri through the tubing. When the solution came into contact with the tubing, the dissolved Tygon acted as a bonding agent to adhere the CuBTTri. It was challenging to design a method to uniformly adhere the small solid MOF particles, as they are not synthesized with a perfectly consistent particle size, and it is difficult to suspend them in solution. Therefore, several of the attempts displayed agglomeration or settling of the particles. Two concentrations of MOF were used and compared, 1.0% w/v and 0.1% w/v. In general, the 1.0% w/v formulation could not be coated uniformly whereas the MOF particles were evenly dispersed using the 0.1% w/v formulation. The distribution of the particles is important, as this would permit dispersed NO generation to inhibit platelet function on the entire blood-contacting surface. Next, the stability of the coating was evaluated under fluid flow. Two aspects were tested using a saline flow circuit with standard ECMO flow rates (1.5 L/min – 2.5 L/min), the stability of the polymeric coating itself and the stability of the CuBTTri. Scanning electron microscope images taken along the surface proved that no delamination or damage occurred to either of the polymeric coatings. To test the stability of the CuBTTri, the copper concentration of the saline was measured during flow experiments. If the CuBTTri is not stable, it would degrade into copper ions and the organic ligand, H₃BTTri. The data was highly variable for the 0.1% w/v formulation during 72 h fluid flow; it is possible that during fluid flow, either the CuBTTri degraded or unreacted copper ions from the synthesis were exposed. Future experiments would be beneficial to determine which is occurring. Time-of-flight mass spectrometry can be used to confirm the presence of the ligand, H₃BTTri which would indicate that the MOF is degrading. For the 72 h flow using the 1.0% formulation, the copper concentration did not change during the experiment, providing confidence that the application can be safe. Finally, the CuBTTri was shown to actively generate NO in the presence of *S*-nitrosoglutathione (GSNO). Interestingly,

the NO flux produced from each of the formulations was approximately equivalent. Originally, I would have expected the 1.0% w/v formulation to produce a higher NO flux because it contains more copper. I hypothesize that only a small amount of copper is exposed on the surface of the tubing for each application. The remainder of the CuBTtri particles would be completely embedded into the polymer, and not exposed to the surface. Using these results, I conclude that the 0.1% w/v formulation is superior because it uses a significantly less amount of CuBTtri, making it less expensive, while providing equivalent NO flux.

Initial coagulation tests performed using an *ex vivo* circuit showed the coating caused no adverse effects toward blood and the coagulation of the blood was not disrupted. However, because of the nature of *ex vivo* blood, we are unable to determine if endogenous RSNOs could react with the CuBTtri to generate NO. Furthermore, members from the Autonomous Reanimation and Evacuation Program are currently conducting *in vivo* experiments. These tests will further assess the hemocompatibility of the CuBTtri coating and will allow us to determine if the RSNOs present within live animals interact with the CuBTtri to generate NO. These *in vivo* experiments could also be used to further verify the safety of the coating with alternate toxicity studies.

3. Conclusions and Future Work for the Oxygenator

Similarly, the goal for the fibers on the oxygenator was to engineer a coating that is uniform, stable, and active. A different polymer (polydopamine) and procedure were used to immobilize the CuBTtri particles on the surface of the fibers. In short, the polydopamine was coated onto the fibers then the CuBTtri was immobilized on the polydopamine surface. Optimizing this method took many iterations as the concentration and amount of polydopamine greatly affected the adhesion of the CuBTtri particles. The final iteration produced a coating

with dispersed CuBTTri across the surface of the fibers. To test for the stability of the coating, the fibers were agitated in a saline solution. There were no signs of delamination or damage to the coating, but a small amount of excess copper was present in the saline after the stability tests. This study along with the inconsistent results seen with the coated tubing raises stability questions regarding CuBTTri in dynamic solutions. I believe an important next step in this project is to perform further dynamic stability tests to determine if CuBTTri is able to withstand the shear forces in ECMO, as the stability of this MOF is essential in determining the safety of this coating. The final results proved the CuBTTri on the surface of the fibers is catalytic activity including after stability tests. NO was generated within the endogenous NO flux produced by the endothelium.

Besides MOF stability tests, future steps for this application include determining if the coating affects gas exchange within the fibers and or causes any adverse effects within blood. It is critical that this device is able to add oxygen and remove carbon dioxide to mimic pulmonary activity, so the polydopamine should not impair this function. Afterward, the application would benefit from blood exposure and *ex vivo* tests can be performed to determine if the coating has an effect on blood.

Throughout this project, I have shown the ability to coat the surfaces of ECMO with CuBTTri. Both applications are in their initial stage but show promise to be safe and effective. After future testing and possibly further modifications, hopefully these coatings can be applied to improve the efficacy of ECMO while reducing the thrombotic and hemorrhagic complications associated with it.